iScience

CellPress
OPEN ACCESS

Article

Small-molecule TIP60 inhibitors enhance regulatory T cell induction through TIP60-P300 acetylation crosstalk

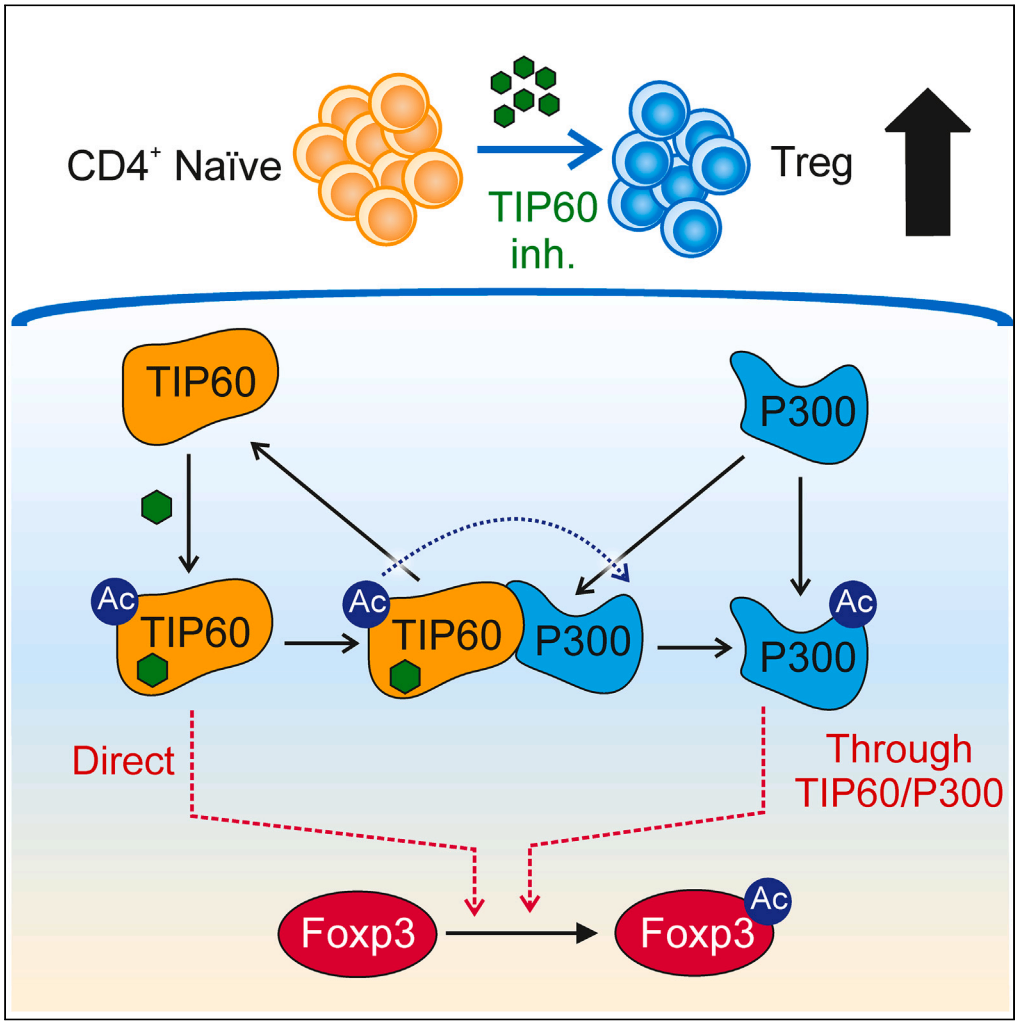

Francisco Fueyo-González, Guillermo Vilanova, Mehek Ningoo, Nada Marjanovic, Juan A. González-Vera, Ángel Orte, Miguel Fribourg

miguel.fribourg@mssm.edu

Highlights

Small-molecule TIP60 inhibitors increase Foxp3 acetylation and Treg induction

An FRET-based method compatible with flow cytometry to follow the acetylation flux

They can activate TIP60 to acetylate P300 thereby increasing Foxp3 acetylation

Fueyo-González et al., iScience *26*, 108491
December 15, 2023
https://doi.org/10.1016/j.isci.2023.108491

iScience

CellPress
OPEN ACCESS

Article

Small-molecule TIP60 inhibitors enhance regulatory T cell induction through TIP60-P300 acetylation crosstalk

Francisco Fueyo-González,[1,2] Guillermo Vilanova,[3] Mehek Ningoo,[1,2] Nada Marjanovic,[4] Juan A. González-Vera,[4,5] Ángel Orte,[4,5] and Miguel Fribourg[1,2,6,*]

SUMMARY

Foxp3 acetylation is essential to regulatory T (Treg) cell stability and function, but pharmacologically increasing it remains an unmet challenge. Here, we report that small-molecule compounds that inhibit TIP60, an acetyltransferase known to acetylate Foxp3, unexpectedly increase Foxp3 acetylation and Treg induction. Utilizing a dual experimental/computational approach combined with a newly developed FRET-based methodology compatible with flow cytometry to measure Foxp3 acetylation, we unraveled the mechanism of action of these small-molecule compounds in murine and human Treg induction cell cultures. We demonstrate that at low-mid concentrations they activate TIP60 to acetylate P300, a different acetyltransferase, which in turn increases Foxp3 acetylation, thereby enhancing Treg cell induction. These results reveal a potential therapeutic target relevant to autoimmunity and transplant.

INTRODUCTION

Regulatory T (Treg) cells are one of the main mediators of central and peripheral tolerance,[1–3] which are key immune processes in transplant, autoimmune disease, and malignancy. A reduction in Treg cell numbers or function is a hallmark of autoimmune disease in animal models[4] and in humans,[5] while increased numbers of Treg cells have been shown to promote murine transplant tolerance and are associated with prolonged transplant survival in humans,.[6,7] Increasing Treg cell frequency in autoimmune disease and transplantation, either by promoting endogenous Treg[8–10] or through autologous Treg transfer,[11,12] constitutes a promising therapeutic endeavor. However, only a few small molecules have been described to promote Treg cells.[13–15]

The transcription factor forkhead box P3 (Foxp3) is the master regulator of the immunosuppressive program in Treg cells.[16] Foxp3 levels in Treg cells are regulated through multiple molecular mechanisms including methylation of the Foxp3 promoter gene region,[17,18] Foxp3 dimerization,[19] as well as Foxp3 post-translational modifications such as cleavage,[20] ubiquitination,[21] and acetylation.[22,23] Of these, Foxp3 acetylation confers stability to the protein and promotes its translocation to the nucleus to induce an immunosuppressive program.[24] Pharmacologically increasing Foxp3 acetylation remains an unmet challenge.

Designing molecules that modulate the activity of acetyltransferases has major therapeutical potential and has been explored extensively in the cancer field.[25–28] TIP60 and P300 are two acetyltransferases described to be involved in the regulation of Foxp3 acetylation. Their Foxp3 acetylating activity has been demonstrated when these proteins were overexpressed in HEK293 cells.[29] It has also been elegantly established in different murine models, including conditional knockouts in Treg cells, that absence of TIP60 and P300 precludes Foxp3 acetylation thereby thwarting Treg cell induction and function.[29–32] A set of small molecules that target the acetyltransferase TIP60 have been described, whose function has been tested in biochemical *in vitro* assays using histones as the substrate. These TIP60 inhibitors vary widely in chemical structure and have been identified either by rational design or through screening,[33,34] but only three of them (NU9056, MG149, and TH1840) are selective for TIP60.[35–37] NU9056, MG149, and TH1840 have shown to reduce TIP60-mediated acetylation of histones at high concentrations and have thus been classified as TIP60 inhibitors. In contrast, we report that these molecules have an unexpected effect in increasing Foxp3 acetylation.

To unravel the mechanism of action of these small-molecule TIP60 inhibitors on Foxp3 acetylation, we used a newly developed Förster resonance energy transfer (FRET)-based methodology to measure protein acetylation compatible with flow cytometry. Combining an *in silico*

[1]Translational Transplant Research Center, Division of Nephrology, Department of Medicine, Icahn School of Medicine at Mount Sinai, New York, NY 10029, USA
[2]Immunology Institute Icahn School of Medicine at Mount Sinai, New York, NY 10029, USA
[3]LaCàN, Universitat Politècnica de Catalunya-BarcelonaTech, 08034 Barcelona Spain
[4]Deparment of Neurology, Icahn School of Medicine at Mount Sinai, New York, NY 10029, USA
[5]Nanoscopy-UGR Laboratory, Departamento de Fisicoquímica, Unidad de Excelencia de Química Aplicada a Biomedicina y Medioambiente, Facultad de Farmacia, Universidad de Granada, Campus Cartuja, 18071 Granada, Spain
[6]Lead contact
*Correspondence: miguel.fribourg@mssm.edu
https://doi.org/10.1016/j.isci.2023.108491

mechanistic computational model with experiments in murine and human Treg induction cultures, we identified a previously unrecognized indirect mechanism by which TIP60 inhibitors increase P300-mediated Foxp3 acetylation to increase Treg cell numbers.

RESULTS

TIP60 inhibitors enhance Treg cell induction

We first decided to explore the effect in murine Treg cell induction cultures of the three selective TIP60 small-molecule inhibitors: NU9056, MG149, and TH1834 (Figure 1A). We isolated naive splenic $CD4^+$ T cells (defined as $CD44^{lo}$ $CD62^{hi}$ purity >95%) from wild-type C57BL/6 (B6) animals, cultured them for 5 days with αCD3/αCD28 activating beads under Treg cell polarizing conditions (IL-2 and TGFβ) in the presence of either vehicle or increasing concentrations of the inhibitors (Figure 1B), and measured using flow cytometry the frequency of $Foxp3^+$ cells (Treg) at the end of the culture.

tIn contrast with TIP60's described acetylating activity on Foxp3,[29,30] all three TIP60 inhibitors showed a dose-dependent increase in the number of $Foxp3^+$ cells at the end of the cultures (Figures 1C–1E), starting at 0.1 μM and reaching their maximum effect at 20–25 μM (NU9056 1.8-fold increase at 20 μM, MG149 2.3-fold increase at 25 μM, TH1834 2.6-fold increase at 25 μM) (Figure 1E). At higher concentrations, the fraction of apoptotic cells in the culture significantly increased (Figure S1A) and cellular viability started to decline (Figure S1B). Of note, at the level of maximum Treg induction enhancement the number of cells at the end of the culture remained stable, i.e., the number of Treg did not decrease (Figure S1C), and the expression of the gene encoding for TIP60 (*Kat5*) remained unaffected. (Figure S1D).

To verify that $CD4^+Foxp3^+$ T cells induced in the presence of TIP60 inhibitors retain the ability to suppress effector T cells, we performed *in vitro* suppression assays. We induced $Foxp3^+CD4^+$ T cells in the presence or absence of MG149 culturing $CD4^+$ naive T cells from *Foxp3*-GFP animals. After confirming the MG149-mediated increase in $Foxp3^+$ cells, we sorted Foxp3-GFP^+ cells by flow cytometry. We then assessed their ability to suppress the proliferation of conventional T (Tconv) cells labeled with a proliferation dye and stimulated in the presence of αCD3/αCD28. These assays demonstrated that $Foxp3^+CD4^+$ T cells induced in the presence of MG149 (20 μM) exhibit a similar suppressive capacity to those induced in the absence of the TIP60 inhibitor (Figure 1F).

These results indicate that small molecules targeting TIP60 can enhance Treg cell induction without affecting their suppressive function.

TIP60 inhibitors increase HAT and KAT activity at low-mid concentrations

Even though TIP60 acetylates multiple substrates, including Foxp3,[38] studies of the inhibitory effects of NU9056, MG149, and TH1834 have been limited to cell lines and *in vitro* biochemical assays evaluating their acetyltransferase activity on histones (histone acetyltransferase, HAT activity) performed at high concentrations (mainly 50 μM or higher).[35–37] Our finding that TIP60 inhibitors enhance Treg cell induction prompted us to investigate whether these inhibitors might exhibit differences in activity at lower concentrations or depending on the substrate (i.e., histones versus Foxp3). We first utilized the peptide-based HAT activity *in vitro* biochemical assay previously used to study the effect of these molecules on TIP60's enzymatic activity for an expanded concentration range that includes lower concentrations (0, 1, 10, 100, 1000, and 2000 μM). This assay detects the colorimetric change of a dye, tetrazolium. In addition, it requires (i) a histone peptide sequence (amino acids 1–23 from histone 3), (ii) the enzyme NADH reductase, (iii) its cofactor acetyl-CoA, and (iv) the acetyltransferase enzyme of interest (here, TIP60 recombinant protein). As TIP60 recognizes the peptide sequence and transfers the acetyl group from acetyl-CoA to the peptide, the NADH reductase is activated, triggering the tetrazolium dye oxidation. This oxidation produces a colorimetric change, which can be measured using a spectrophotometer (Figure 2A). Consistent with our hypothesis of the concentration-dependent dual effects of these molecules, the results using this assay with only TIP60 protein present indicate that all three molecules increase TIP60 HAT activity at low-mid concentrations (1–100 μM) and decrease it at high concentrations (1–2 mM) (Figure 2B).

To study whether TIP60 inhibitors had the same effects on Foxp3 acetylation, we adapted the HAT assay to measure Foxp3 acetylation. We did this by replacing the histone peptide substrate with a sequence spanning the two lysines in positions 262 and 267 of the Foxp3 protein known to be acetylated by acetyltransferases TIP60 and P300 and conserved between human and murine Foxp3.[39] We will refer to the Foxp3-adapted assay as the lysine acetyltransferase (KAT) assay. Our results indicate an analogous dose-dependent dual effect of the TIP60 inhibitors on TIP60 acetyltransferase activity on Foxp3 but a less pronounced inhibitory effect (Figure 2C).

To ensure that these inhibitors acted selectively on TIP60 and not on P300, we compared the effects of TIP60 inhibitors using our KAT assay with the TIP60 or the P300 protein. Compared at the same concentration and in the absence of inhibitors, P300 acetylated the Foxp3 peptide approximately twice as much as TIP60 (Figure 2D). In contrast, with the addition of TIP60 inhibitors at low-mid concentrations (NU9056 at 20 μM, MG149 and TH1834 at 25 μM), we only observed an increase in TIP60 acetyltransferase activity. Consistently, addition of a P300 inhibitor (C646 at 20 μM) only affected P300's ability to acetylate its substrate demonstrating that NU9056 MG149 and TH1834 selectively modulate TIP60 acetyltransferase activity (Figure 2E). TIP60 has been described to autoacetylate, i.e., one molecule of TIP60 can acetylate another TIP60 molecule thereby increasing its acetyltransferase activity.[40] We further performed western blot analyses of the acetylation of the TIP60 protein in our biochemical assay in the presence of the TIP60 inhibitors. Our results revealed that these molecules increase TIP60 acetylation at low-mid concentrations and either not affect or decrease it at high concentrations (Figure S2) consistent with the effects observed on the peptidic substrates.

Together these results support the idea that NU9065, MG149, and TH1834 are not TIP60 inhibitors but rather TIP60 modulators that enhance the enzyme's direct acetyltransferase activity on Foxp3 at low-mid concentrations and inhibit it at high concentrations.

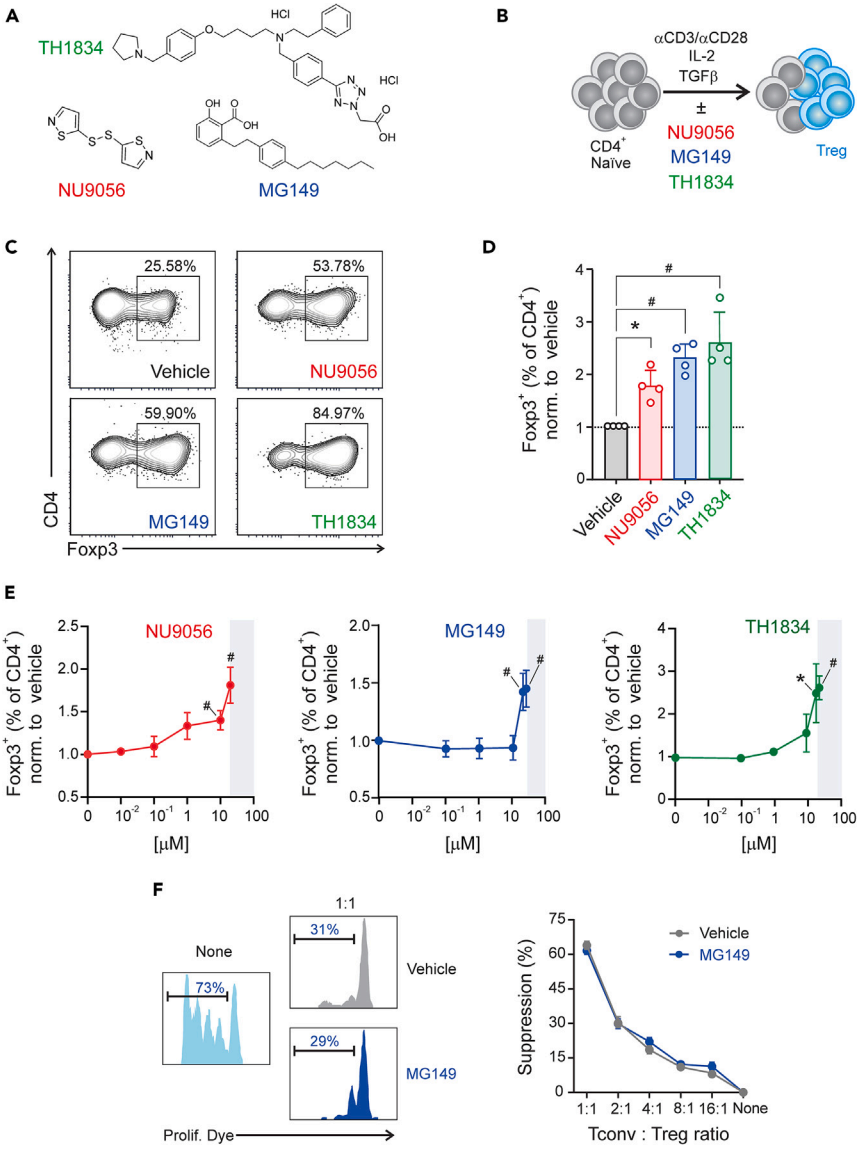

Figure 1. TIP60 inhibitors enhance Treg cell induction

(A) Molecular structures of TIP60 inhibitors NU9056, MG149, and TH1834.

(B) Description of experimental Treg cell induction cultures in the presence of TIP60 inhibitors and controls.

(C) Representative scatterplots and gating strategy obtained at the end of Treg cell cultures treated with NU9056 (20 μM), MG149 (25 μM), TH1834 (25 μM) or vehicle, and (D) summary results.

(E) Dose-response curves of the Treg cell-induction enhancing effect. Gray shading indicates concentrations at which viability was <95% (see Figure S1) (mean ± SEM, n = 4–8 per group, three independent experiments, ANOVA with post-hoc Tukey HSD test, *p < 0.05, #p < 0.01, differences in E are in comparison to vehicle).

(F) Representative histograms and results summary of the suppression capacity of Treg cells induced in the presence of vehicle or MG149. Suppression capacity was calculated as the relative decrease in proliferation in the presence of Treg cells (comparisons at each Tconv: Treg ratio were non-significant; mean ± SEM, n = 3 of three independent experiments ANOVA with post-hoc Tukey HSD test).

An FRET-based technique to measure Foxp3 acetylation in Treg cells

We hypothesized that TIP60 inhibitors enhance Treg cell induction by increasing Foxp3 acetylation. To test this hypothesis, we first used a proximity ligation assay (PLA), which we and others have successfully used to measure Foxp3 acetylation.[41,42] We set up Treg cell induction cultures treated with vehicle or NU9056 (20 μM) and compared the levels of Foxp3 after 5 days. Consistent with our hypothesis, when compared with vehicle, cells cultured with NU9056 showed increased levels of Foxp3 acetylation (Figure 3A).

Despite being the current state-of-the-art to measure Foxp3 acetylation *in situ* (i.e., not using cell lysates and western blot), PLA has strong limitations: (i) it is a semiquantitative method that requires the amplification of a nucleotide sequence, and (ii) it mainly relies on microscopy

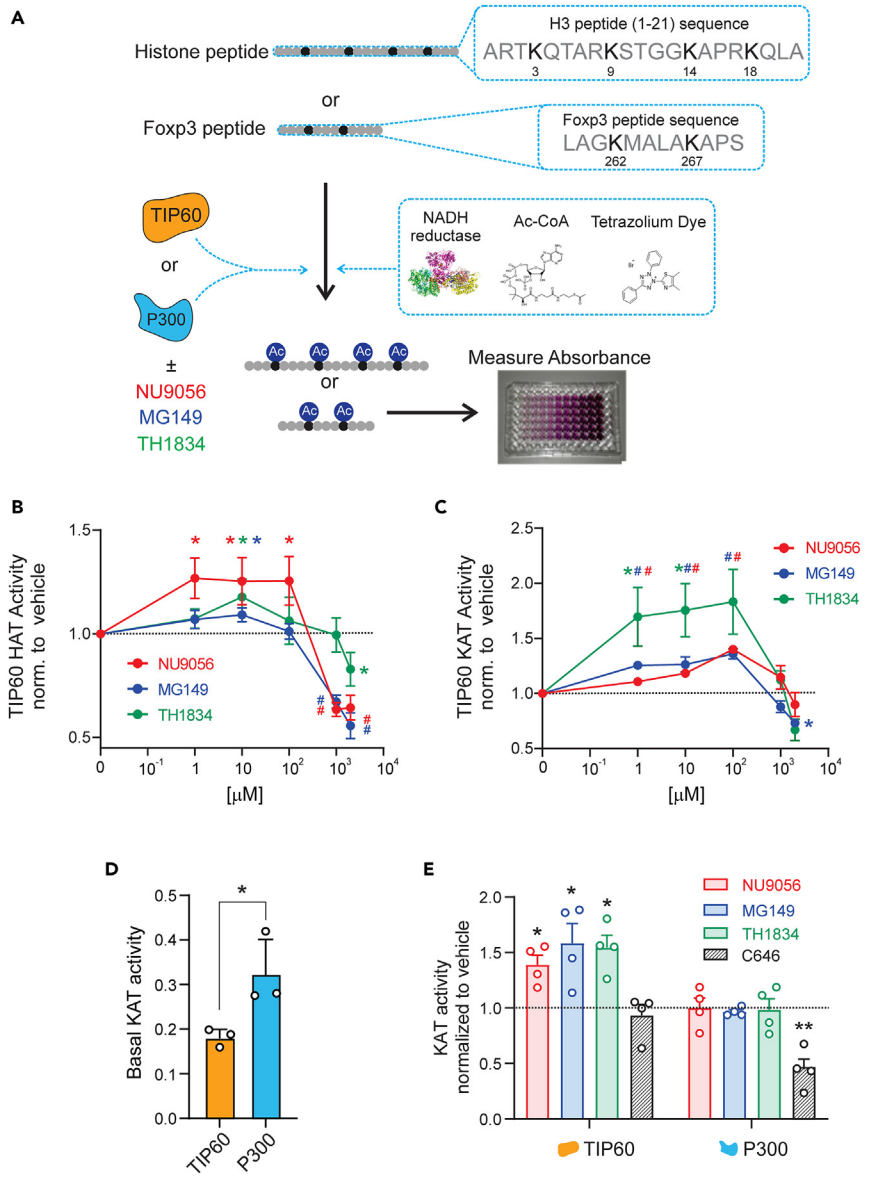

Figure 2. TIP60 inhibitors increase HAT and KAT activity at low-mid concentrations

(A) Description of the peptide-based assay to determine TIP60 histone acetyltransferase (HAT) and Foxp3 lysine acetyltransferase (KAT) activities.

(B and C) Dose-response curve for the effect of TIP60 inhibitors NU9056, MG149, and TH1834 on TIP60 B HAT and C KAT activities.

(D) Baseline TIP60 and P300 KAT activity on Foxp3 and (E) differential effect of TIP60 inhibitors and P300 inhibitor C646 (20 μM) on P300 and TIP60 KAT activity (mean ± SEM, n = 3–5 from at least two independent experiments, B, C, and E one-way ANOVA followed by Tukey post-hoc test, all comparisons with normalized baseline; D mean ± SEM, t-test; *p < 0.05, #p < 0.01).

which only allows assessing a limited number of cells. Thus, PLA is not well adapted to study Treg cells, which constitute only a fraction of the cells in the culture (see Figure 1C). To overcome these limitations, we developed a FRET-based method to quantify protein acetylation, which (i) is compatible with different instruments, including flow cytometry and fluorescent microscopy, (ii) is versatile and allows us to measure protein acetylation in different subpopulations, and (iii) is easily scalable to a large number of samples.

In our FRET-based approach, we stain cells with two antibodies labeled with fluorophores selected based on their spectral overlap: an antibody against Foxp3 conjugated to a donor fluorophore (Alexa Fluor 488, AF488 which recognizes amino acids 75–125 of the mouse Foxp3 protein, see STAR Methods) and a second antibody that binds to all acetylated lysines conjugated to an acceptor fluorophore (Alexa Fluor 555, AF555). When the donor fluorophore is excited by 488 nm visible light, its excitation energy may be transferred through FRET to the acceptor, triggering its emission, provided the two fluorophores are in close proximity (<10 nm, given the Förster distance, R_0, for the proposed FRET pair is approximately 7 nm[43]) (Figure 3B). Hence, we can use the extent of the sensitized FRET signal as a measure of the degree of

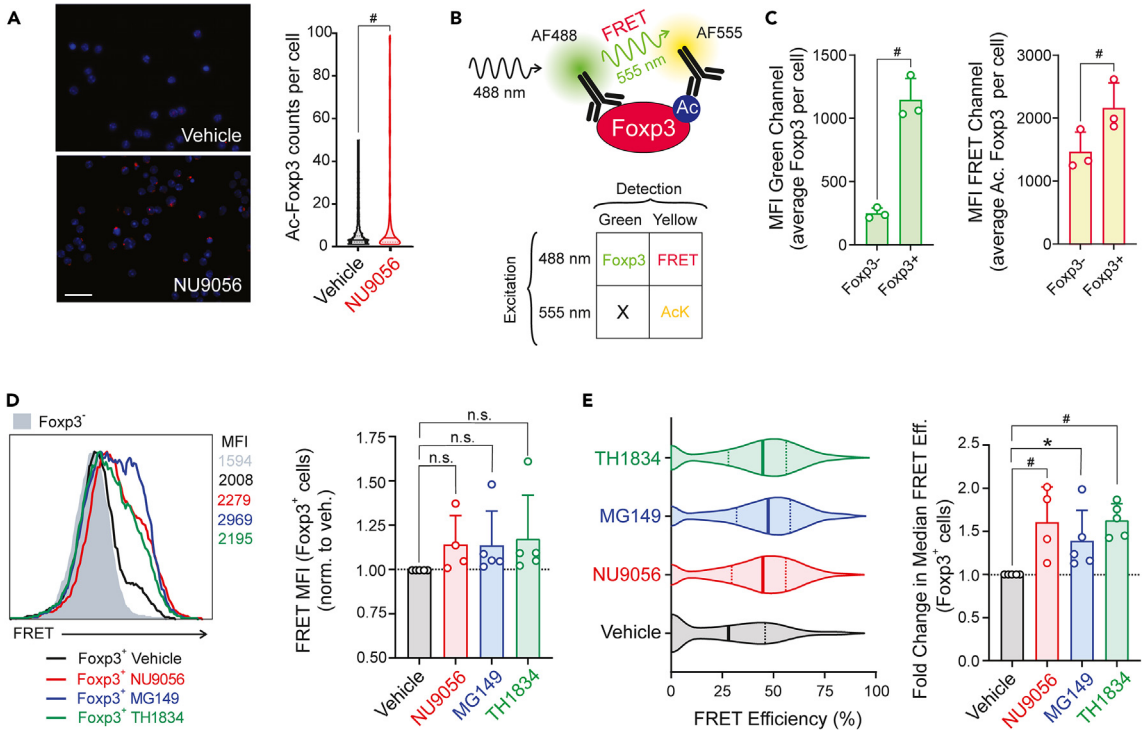

Figure 3. A FRET-based technique to measure Foxp3 acetylation in Treg cells

(A) Representative image and violin plots depicting the distribution of Foxp3-acetylation by proximity ligation assay (PLA) (solid line represents the median, dotted lines indicate quartiles, n = 394–480 cells per group from three independent experiments, only cells with at least one spot included; #$p < 0.01$, Mann-Whitney test).

(B) Description of the FRET-based flow cytometry strategy to measure Foxp3 acetylation.

(C) Green channel and FRET channel mean fluorescence intensities (MFI) in Foxp3$^-$ and Foxp3$^+$ cells at the end of Treg cell cultures as described in Figure 1 (n = 3, from 2 independent experiments, t test,*$p < 0.05$, #$p < 0.01$, see also Figure S1 for controls).

(D) Representative histograms depicting the FRET channel signal intensity in the Foxp3$^+$ compartment at the end of Treg cell induction cultures treated with NU9056, MG149, and TH1834 (20 μM) or vehicle and summary results.

(E) Representative violin plots depicting the distribution of FRET Efficiency per cell (see STAR Methods for details) in Foxp3$^+$ cells in the same cultures and statistical summary of the results (D and E summaries depict mean ± SEM, n = 4–5 of three independent experiments, ANOVA followed by Tukey post-hoc test, *$p < 0.05$, #$p < 0.01$).

Foxp3 acetylation selectively in CD4$^+$ Foxp3$^+$ cells (Treg cells, identified based on the donor signal) (Figures 3C and S1). We can thus obtain the degree of acetylation per cell (FRET intensity value in each cell) as well as the average signal in the Foxp3+ compartment by measure the mean fluorescence intensity (MFI). Furthermore the apparent FRET efficiency per cell typically used in microscopy experiments[44,45] and defined as %FRET (intensity of the acceptor*100/(intensity of the acceptor + intensity of the donor), can also be calculated in flow cytometry experiments. This measurement is less sensitive to noise and is corrected for spectral bleed-through in each channel using the corresponding singly-stained controls (see STAR Methods).

Using the FRET-based method, we measured Foxp3 acetylation at the end of Treg cell induction cultures in the presence of vehicle or NU9056, MG149, and TH11834. Consistent with the results obtained with PLA (Figure 3A), we observed an increase in FRET signal (Figure 3D) and FRET efficiency (Figure 3E, less sensitive to noise and is thus less variable) in the CD4$^+$Foxp3$^+$ compartment at the end of Treg cell induction cultures.

Together, our results indicate that we can (i) successfully use a FRET-based technique to measure protein acetylation in thousands of CD4$^+$Foxp3$^+$ cells using flow cytometry and (ii) target TIP60 with small molecules to enhance Foxp3 acetylation.

Computational prediction of a P300-dependent mechanism of action of TIP60 inhibitors

We decided to investigate whether the increased TIP60 activity and the direct effects on Foxp3 observed in our peptide-based assay (Figure 2) could be enough to explain the dramatic increase in Foxp3$^+$ cells at the end of the Treg induction cultures (Figure 1) In addition to its direct acetylating effect, TIP60 has been postulated to act in a concerted manner with P300 to increase Foxp3 acetylation.[29] However, the mechanism underlying this interaction remains to be elucidated. We used an *in silico* approach to generate hypotheses regarding the potential contribution of TIP60 inhibitors (NU9056, MG149, and TH1834) to this concerted mechanism. We built an ordinary differential equation

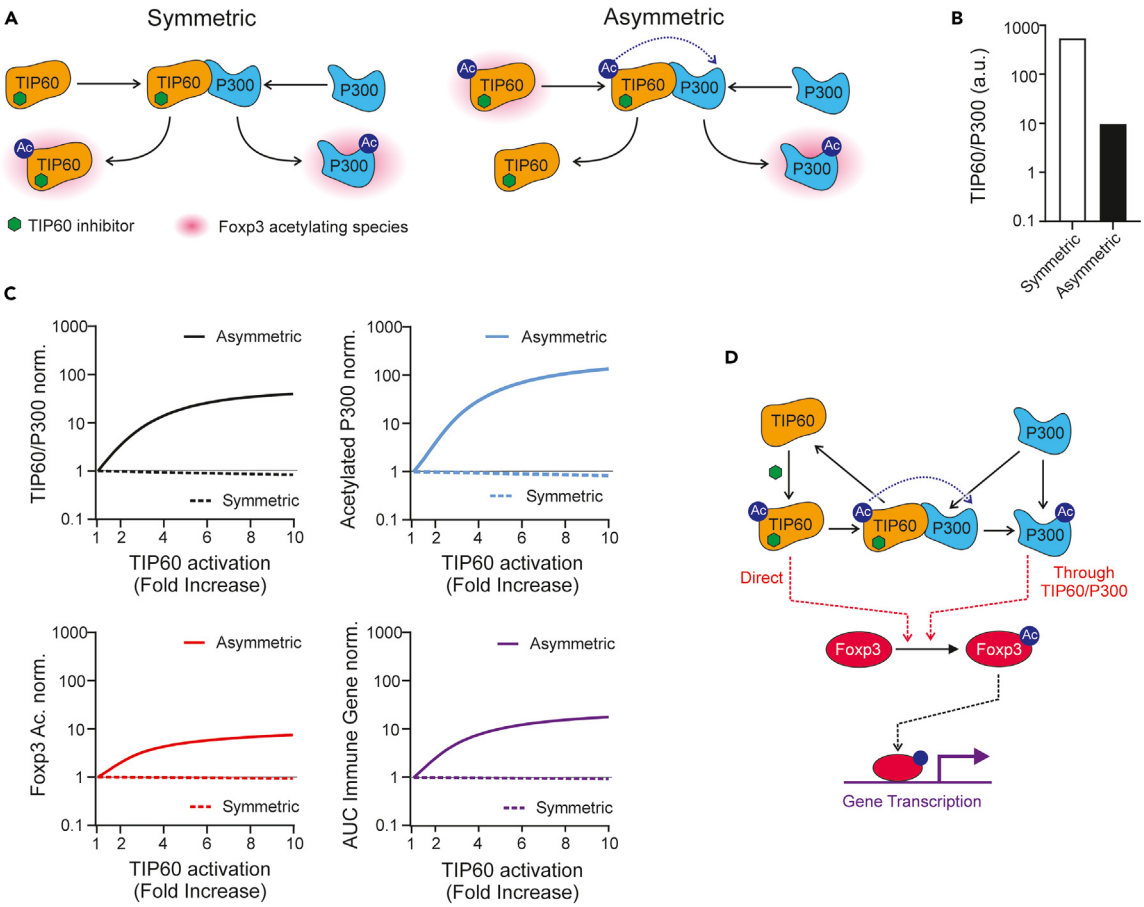

Figure 4. Computational prediction of a P300-dependent mechanism of action of TIP60 inhibitors

(A) Diagram depicting the symmetric and asymmetric computational models tested to ascertain a potential modulatory mechanism of P300 activity by TIP60 inhibitors through TIP60/P300 heteromer formation.

(B) Extent of TIP60/P300 heteromer formation once the symmetric and asymmetric versions of the model have reached a steady state.

(C) Computational simulations of the effect of TIP60 activation on TIP60/P300 heteromer formation, acetylated P300, acetylated Foxp3, and transcription of a representative immune gene by Foxp3 (see Data S1 for details). Values are normalized to the corresponding asymmetric and symmetric baseline values (steady state).

(D) Proposed direct and P300-dependent acetylation fluxes that lead to Foxp3 acetylation in Treg and the mechanism of action of TIP60 inhibitors that result in their increase.

(ODE) mechanistic model of Foxp3 acetylation that includes direct acetylation of Foxp3 by TIP60 and P300, as well as different modes of interaction between P300 and TIP60 (see details Data S1).

Acetyltransferases are promiscuous and acetylate other acetyltransferases in the cell. In most cases, acetylation enhances their acetyltransferase activity.[46–49] As mentioned previously, our *in vitro* results using TIP60 in its active form indicate that TIP60 inhibitors can enhance its acetyltransferase activity (Figure 2). Through computational simulations, we studied the effect of an increase in TIP60 activity on Foxp3 acetylation in versions of the models with two possible mechanisms for TIP60/P300 interaction: one previously postulated in the literature in which TIP60 and P300 form a complex and mutually acetylate each other (symmetric),[29] and one in which activated TIP60 binds to P300 and acetylates P300 to increase its activity (asymmetric) (Figure 4A). Following findings by other groups, our model incorporates the assumption that P300 acetylates Foxp3 more efficiently than TIP60.[29,31,50,51] Of note, multiple proteins in the cell control the activity of TIP60 and P300, with one of their mechanisms being through acetylation.[52,53] In the models, we lumped these into a single reaction that the TIP60 inhibitors can activate or inhibit (see Data S1 for all model assumptions, complete sensitivity analysis, and all the modes of TIP60/P300 interaction explored).

At steady state (i.e., allowing each model to equilibrate) and in the absence of TIP60 inhibitors, the symmetric model predicts a higher degree of TIP60/P300 complex formation (Figure 4B). These differences are due to the complete reliance of Foxp3 acetylation on the formation of the TIP60/P300 complex in the symmetric model. Strikingly the model predicts that TIP60 inhibitors exploit the asymmetry of the model, and their enhancing of TIP60 activity in the asymmetric model results in a sharp increase in TIP60/P300 formation, acetylated P300, acetylated Foxp3, and subsequent Foxp3-mediated gene induction in the simulations. In contrast, all these features slightly decrease in the symmetric case upon TIP60 activation (Figure 4C).

Our previous experimental findings indicate that NU9056, MG149, and TH1834 increase Foxp3 acetylation in Treg cell induction cultures (Figure 3), which the asymmetric model would support. Mechanistically, the asymmetric *in silico* model posits that although TIP60 inhibitors enhance the direct effect of TIP60 on Foxp3 acetylation, their effects on Foxp3 acetylation are mainly driven by an increase in affinity of acetylated TIP60 for P300. In turn, this favors TIP60/P300 heteromer formation, acetylation of P300 by TIP60, and subsequent increase in Foxp3 acetylation (Figure 4D). In the following sections, we experimentally assess the postulated contribution of this P300-mediated mechanism to the increase in Foxp3 acetylation and enhancement of Treg induction by TIP60 inhibitors.

TIP60 inhibitors modulate P300 acetyltransferase activity on Foxp3

To test the P300-dependent molecular mechanism proposed by our computational model, we first explored whether TIP60 inhibitors increased TIP60/P300 interactions in our Treg cell induction cultures. To measure these interactions, we adapted our FRET-based method by using antibodies recognizing TIP60 and P300 (Figure 5A), which allows us to detect the formation of the heterodimer. Our results indicate that the treatment of Treg cell induction cultures with NU9056, MG149, and TH1834 at low-mid concentrations (maximum Treg enhancing effect while preserving viability, see Figure 1) increased the TIP60/P300 FRET signal and the average FRET efficiency per cell in the Foxp3$^+$ subpopulation consistent with an increase of TIP60/P300 complex formation (Figures 5B and S4A).

P300 and TIP60 have been postulated to acetylate each other as part of their interaction with Foxp3 based on results in cell-lines and full deletion studies *in vivo*.[29–32] To unravel the flux (direct vs. through P300 modulation) of acetylation in primary T cells (Figure 4D), we measured at the end of our Treg cell induction cultures the changes in TIP60 acetylation, TIP60/P300 heteromer formation, and P300 acetylation elicited by the TIP60 modulator MG149, in the presence or absence of a small molecule that inhibits the catalytic site of P300 and prevents it from acetylating its substrates (C646).[53,54] We measured P300 and TIP60 acetylation using an analogous FRET-based approach to that used to measure Foxp3 acetylation (Figure 3) in which we swapped the AF488-bound α-Foxp3 antibody with antibodies that recognize P300 and TIP60, respectively.

We first identified a dose of C646 that would not completely abrogate Treg cell formation in the culture. C646 exclusively inhibited Treg induction in a dose-dependent manner in our culture, and completely abrogated Foxp3$^+$ formation at 25 μM (Figure S4B). Treatment with MG149 (25 μM) increased the percentage of Foxp3$^+$ cells at the end of the cultures, but this effect disappeared in the presence of a medium dose of C646 (1 μM, associated with 40% reduction in Treg induction Figure S4B). C646 alone reduced the percentage of Foxp3$^+$ cells, consistent with the strong dependence of Foxp3 acetylation on P300[41,50] (Figure 5C).

Consistent with the predicted acetylation sequence for the TIP60/P300 effect by the computational model (Figure 4D), in our experiments MG149 increased TIP60 acetylation, TIP60/P300 heteromer formation, P300 acetylation, and Foxp3 acetylation. Of note, in the presence of MG149 at 25 μM combination of TIP60 with P300 in our *in vitro* assay also increased the Foxp3 peptide acetylation when compared to TIP60 alone (35.43 $\pm$ 0.10% increase; p value = 0.029). Blocking P300's ability to acetylate its substrates did not affect the levels of acetylated TIP60, TIP60/P300 heteromer, and acetylated P300 (Figures 5D and 5E). Instead, these were driven by the presence (increase) or absence of TIP60 inhibitor (compared to baseline), suggesting that TIP60 inhibitors enhance P300 acetylation through the TIP60/P300 heteromer. At the medium dose used (1 μM), C646 alone only partially reduced Foxp3 acetylation, consistent with a direct contribution of TIP60 on Foxp3 acetylation (Figure 5F). Supporting our hypothesis that TIP60 inhibitors enhance both the direct and P300-dependent mechanisms, in cells treated with MG149 + C646 (Figure 5E) we observed a 2-fold increase in Foxp3 acetylation compared to that of cells treated with C646 alone (Figure 5F). Interestingly, C646 alone reduced TIP60/P300 formation suggesting that P300 acetylation might play a role in its formation/stabilization in the absence of inhibitors. We next performed immunoprecipitations with antibodies recognizing TIP60, P300, and Foxp3 from cell lysates at the end of Treg induction cultures in the presence or absence of MG149 (25 μM, a concentration that did not affect viability, see Figure S1), and blotted with an antibody that recognizes acetylated lysines. MG149 increased TIP60, P300, and Foxp3 acetylation (Figure 6), consistent with the FRET-based method results, further validating our findings.

Together, these results support the hypothesis put forward by the computational model (Figure 4C) that TIP60 inhibitors exert most of their effect through a TIP60-mediated increase of P300 acetyltransferase activity on Foxp3.

TIP60 inhibitors enhance Treg cell induction in human cells

Given our results in murine cells, we decided to explore whether the TIP60 inhibitors could also enhance human Treg cell inductions. We set up analogous Treg cell induction culture experiments by isolating CD4$^+$ naive T cells (CD45RA$^+$CD45RO$^-$, >95% purity assessed by flow cytometry) from peripheral blood mononuclear cells (PBMCs) and culturing them with αCD3/αCD28 activating beads under Treg cell polarizing conditions (IL-2 and TGFβ) in the presence or absence of TIP60 inhibitors (NU9056, MG149, and TH1834) (Figure 7A). Consistent with our findings with murine cells (Figure 1) all three TIP60 inhibitors increased the number of Foxp3$^+$ cells at the end of the Treg cell cultures (Figure 7B). The FRET-based approach revealed an analogous molecular mechanism responsible for their Treg cell induction enhancement that increased TIP60 acetylation, heteromer formation, P300 acetylation, and Foxp3 acetylation (Figures 7C and S4D). When compared with murine cultures (Figure 5), the effect on Treg induction was moderate, which was concomitant with a higher increase in TIP60/P300 heteromer and lower P300 acetylation, suggesting that higher levels of heteromerization might be required in human cells to achieve the increase in P300 acetylation.

To further confirm the effect of TIP60 inhibitors on Foxp3 acetylation, we employed the FRET-based assay in confocal microscopy at the end of Treg cell induction cultures treated with or without MG149. Unlike flow cytometry, confocal microscopy does not allow us to analyze

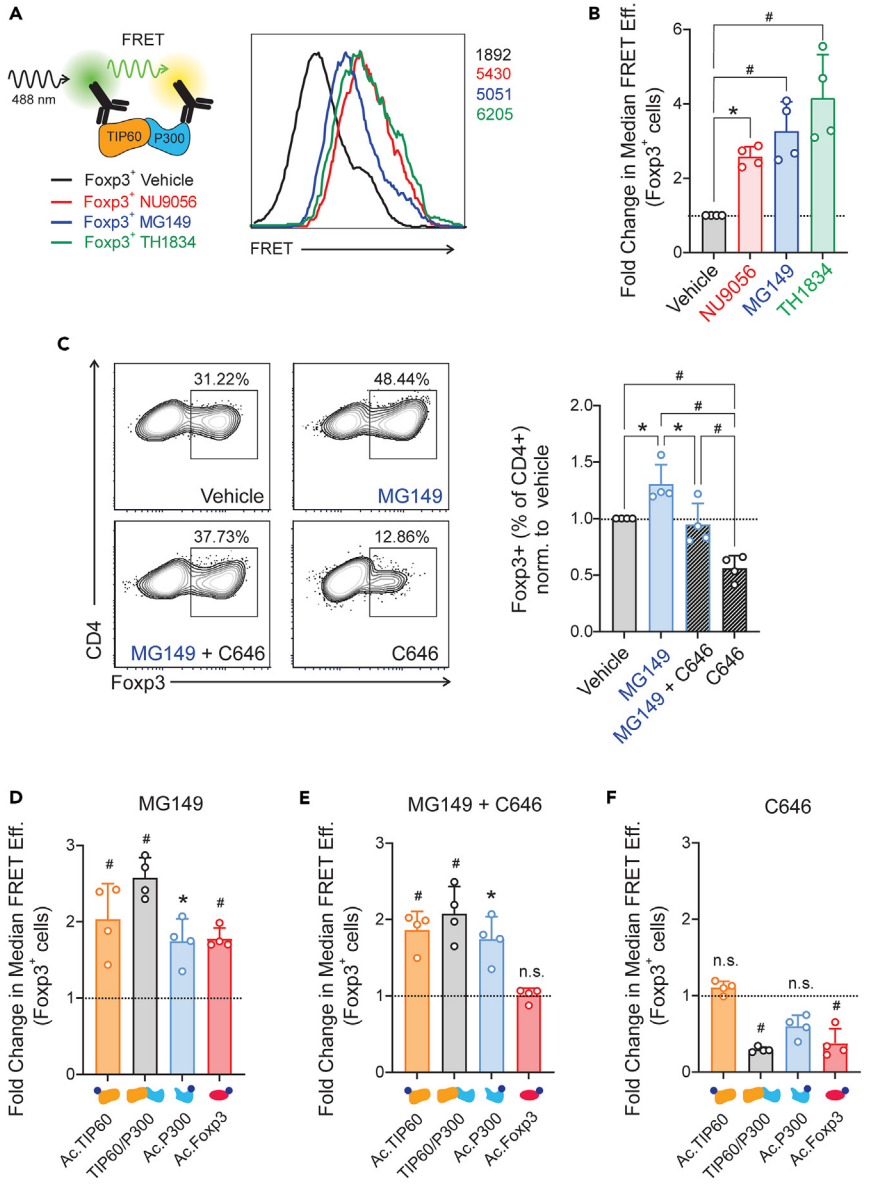

Figure 5. TIP60 inhibitors modulate P300 acetyltransferase activity on Foxp3

(A) FRET-based strategy to measure TIP60/P300 heteromer formation and representative histograms indicating FRET signal in CD4$^+$ Foxp3$^+$ cells from Treg cell induction cultures treated with or without TIP60 inhibitors (NU9056 20 μM, MG149 and TH1834 25 μM) and (B) FRET-Efficiency summary results.

(C) Representative scatterplots and summary results indicating the percentage of Foxp3$^+$ cells at the end of Treg induction cultures in the presence of MG149 (20 μM), C646 (1μM), or MG149 + C646.

(D–F) Summary results of TIP60 acetylation, TIP60/P300 heteromer formation, P300 acetylation, and Foxp3 acetylation measured by FRET (FRET Efficiency) in identical cultures treated with MG149 (D), MG149 + C646 (E) or C646 alone (F). (Bar graphs depict mean ± SEM, n = 4 from three independent experiments. ANOVA followed by post-hoc Tukey HSD test. (D–F) The ANOVA was performed for the same FRET pair across Vehicle, MG149, C646, and MG149 + C646 groups and all comparisons referred to vehicle; *p < 0.05, #p < 0.01).

thousands of cells. However, such microscopy experiments provide an extremely sensitive and direct visualization of individual cells. For this analysis, we collected > 7 images of different fields of view containing several cells. In each image, we selected Foxp3$^+$ cells by applying an intensity threshold to the AF488 channel. Then, we reconstructed the percentage FRET images (Figures 7D and S5) using the same equation employed in flow cytometry experiments. We performed a single-cell analysis of all the collected images using a segmentation procedure implemented in ImageJ. Consistent with our flow cytometry results, we observed an increase in FRET efficiency in cells treated with MG149 compared to vehicle (Figure 7D). This result further emphasizes the versatility and suitability of the FRET-based assay to measure protein acetylation, not only using flow cytometry but also microscopy experiments.

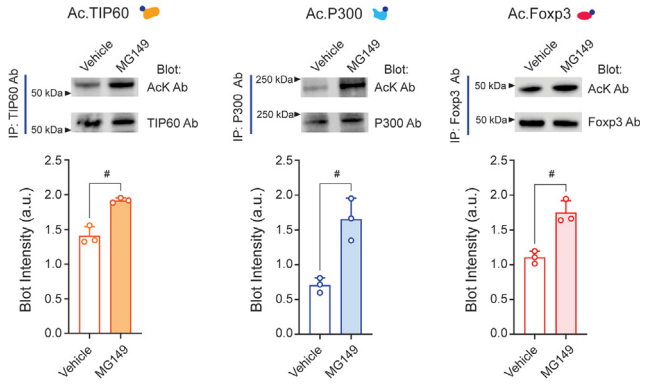

Figure 6. Immunoprecipitation studies

TIP60, P300, and Foxp3 protein was immunoprecipitated from $CD4^+$ $Foxp3^+$ cells from Treg cell induction cultures lysates treated with or without MG149 (20 μM) and blotted with an antibody recognizing acetylated lysines (lanes were loaded with the same amount of protein obtained after immunoprecipitation). Representative blots (top) and quantification (bottom) (ImageJ, see STAR Methods) (mean ± SEM, n = 3 per group, t test, *p < 0.05, #p < 0.01).

Finally, we tested the functionality of human Treg cells induced in the presence of TIP60 inhibitors. Sorted $CD4^+CD25^{hi}CD127^-$ cells from cultures treated with and without MG149 suppressed T cell proliferation with comparable efficiency (Figure 7E), confirming that small molecules that target TIP60 can enhance Treg induction in human cultures by increasing Foxp3 acetylation.

DISCUSSION

In this work, we demonstrate that TIP60 inhibitors increase Foxp3 acetylation in T cells through the modulation of P300 activity and subsequent acetylation of Foxp3, thereby enhancing Treg cell inductions in human and murine cells. We also describe a newly developed FRET-based method to measure acetylation compatible with flow cytometry and microscopy and utilize it to establish the contribution of this mechanism to Foxp3 acetylation.

Given that TIP60 can also directly acetylate Foxp3, the fact that it can modulate the P300-mediated Foxp3 acetylation (and divert the acetylation flux) reveals the crosstalk in terms of signaling between these two pathways. We acknowledge that many proteins, including deacetylases, are involved in modulating the acetylation fluxes in cells that lead to Foxp3 acetylation.[16,30,31,55,56] The studies presented herein contribute to the current knowledge in the field and describe a previously unrecognized mechanism to modulate these fluxes pharmacologically.

Our results reveal that the three small-molecule TIP60 inhibitors (NU9056, MG149, and TH1834) exert a dual effect on TIP60 activity: activation at lower-mid concentrations and inhibition at higher concentrations. Of note, we observed no effects on phosphorylation of TIP60, a marker of activation[57] (data not shown). Although MG149 can inhibit other acetyltransferases, NU9056 and TH1834 have been described to be selective for TIP60 (an MYST acetyltransferase) versus other histone acetyltransferases from both the MYST family (MOF) and other families (P300, and PCAF).[34–37] With the advent of molecular tools to study the mechanism of action of small molecules on protein activity, the complexity of their modulatory effects is being unraveled.[58] One such complex behavior recently being recognized is inhibitor-induced activation.[59] Taking inspiration from these findings, we could postulate the existence of two binding sites as an explanation for the dual behavior of these compounds in TIP60: (i) an activating allosteric site available at lower-mid concentrations, and (ii) an orthosteric site that becomes occupied at higher concentrations. We have generated additional simulations in which we included a reaction in the computational model describing the orthosteric inactivation of TIP60 activity at high concentrations (see Data S1) and recapitulated the dual results obtained in Figure 2, supporting that the allosteric/orthosteric hypothesis is compatible with the results. Notably, the three compounds have significantly different chemical structures. Deciphering whether NU9056, MG149, and TH1834 share orthosteric and/or allosteric TIP60 binding sites will require structural biology studies, which are beyond the scope of this work. These results might shed some light on the paradoxical effects of certain compounds on enzymatic activity reported in the literature.[60,61]

The peptide-based *in vitro* biochemical assay used to study the direct effects of TIP60 on Foxp3 (Figure 2) provides a unique opportunity to study the effects of TIP60 in isolation, using peptides that include the most common acetylation sites described in the literature and shared between mice and humans.[39] Lysines K262 and K267 are outside the leucine-zipper domain in which K249 and K251 (K250 and K252 in humans) are located. As described by Song et al.,[19] this domain is responsible for the oligomerization of Foxp3 and is selectively acetylated by P300. In their experiments, heterologous expression of Foxp3 in Jurkat cells leads to acetylation at other lysines by P300 as well as by other acetyltransferases. We acknowledge that the results in Figure 2 could be due to differences in acetyltransferase activity of TIP60 and P300 on these two lysines. However, our results indicate that this assay successfully predicts the pharmacological properties of NU9056, MG149, and TH1834 in primary T cells and it could be easily adapted to test other acetylation sites in the Foxp3 protein.

To our knowledge, this is the first report of an FRET-based assay to measure acetylation in combination with flow cytometry. We demonstrate that this novel approach can be used to study Foxp3 acetylation in murine and human Treg cells. Furthermore, its flexibility makes it

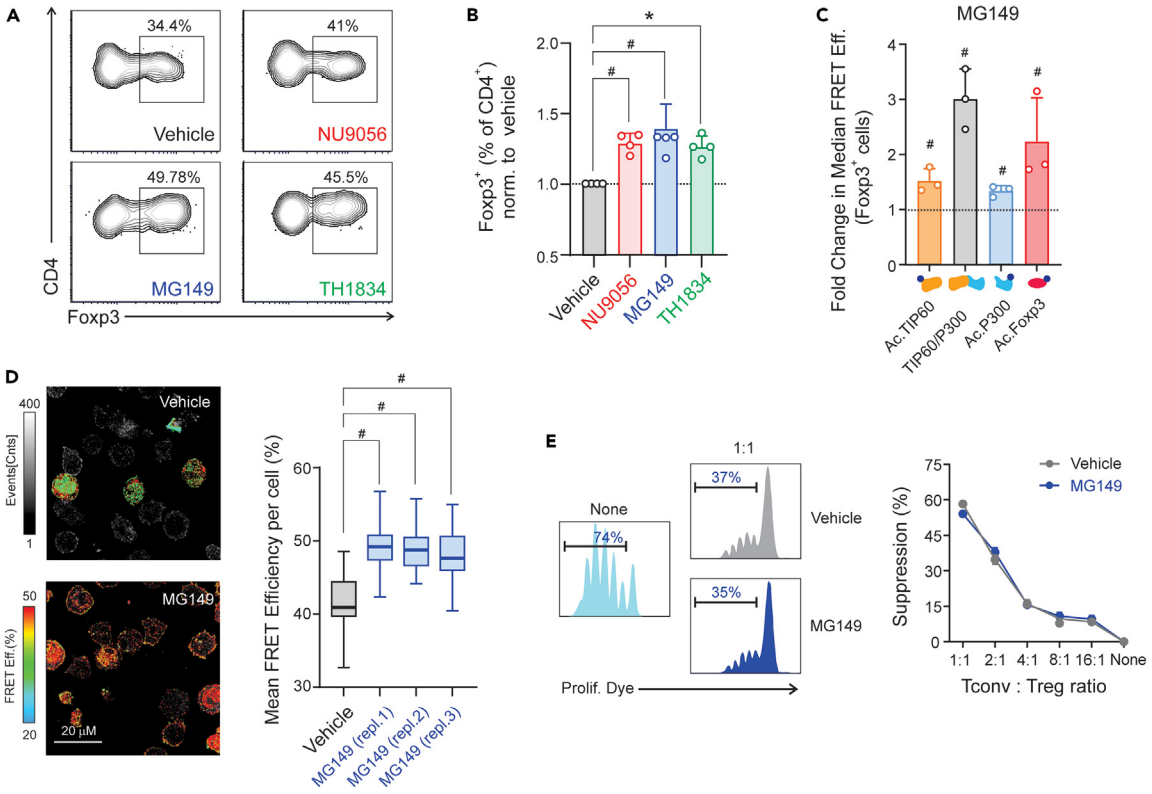

Figure 7. TIP60 inhibitors enhance Treg cell inductions in humans

(A) Representative scatterplots and (B) summary results of Foxp3$^+$ cells at the end of human Treg cell induction in the presence of vehicle, and 10 μM NU9056, MG149, or TH1834.

(C) TIP60 acetylation, heteromer formation, P300 acetylation, and Foxp3 acetylation measured by FRET (FRET Efficiency) in MG149 treated cultures when compared to vehicle (mean ± SEM, n = 3 from three independent experiments, t test for each FRET comparing vehicle and MG149, *p < 0.05, #p < 0.01).

(D) Representative FRET images comparing vehicle and MG149-treated cultures, see also Figure S3, using a pseudocolor scale to indicate the %FRET efficiency; and results of the single-cell segmentation analysis for MG149 treated cultures (3 independent repetitions) compared to vehicle (values in boxes are from at least 7 different images that contain at least 3 different cells in the field of view; mean values are indicated in bold, box size indicates SEM, and whiskers represent s.d.; ANOVA followed by post-hoc Tukey HSD test performed for the MG149 repetitions; all comparisons referred to vehicle. #p < 0.01).

(E) Representative histograms and results summary of the suppression capacity of Treg cells induced in the presence of vehicle or MG149. Suppression capacity was calculated as the relative decrease in proliferation in the presence of Treg cells (comparisons at each Tconv:Treg ratio were non-significant; mean ± SEM, n = 3 of three independent experiments ANOVA with post-hoc Tukey HSD test).

easily adaptable to measure the acetylation of other proteins and even heteromerization (Figure 3). Application of FRET in flow cytometry is limited (i) by a lower signal-to-noise ratio (SNR) than the signal coming from only one fluorophore and (ii) cell autofluorescence, which in the context of microscopy can be addressed using fluorescence life microscopy (FLIM).[62] These two aspects could become limiting if the cellular expression of the molecule under study is low. Studying the role of TIP60 and P300 on Foxp3 acetylation through plasmid expression in cell lines[29] has the advantage of working with increased amounts of protein to perform western blots and co-immunoprecipitations, but might provide a distorted view of the interactions happening in Treg cells. Our FRET-based approach overcomes these limitations and those of the PLA. It allows us to study acetylation in Treg cells by providing seamless integration with flow cytometry and surface markers to analyze multiple subpopulations simultaneously. Our simple approach is powerful for discriminating different acetylation states, although an in-depth study of the specific acetylation sites would require more intricate techniques and analysis, such as mass spectrometry.[63]

Recently published work has reported that two small molecule compounds that bind to TIP60 without affecting its catalytic activity (referred to by the authors as allosteric modulators) can restore Foxp3-TIP60 interactions lost in Treg cells through the most common Foxp3 gene mutations in immunodysregulation polyendocrinopathy enteropathy X-linked syndrome (IPEX).[32] Our findings propose an additional mechanism through which targeting TIP60 can enhance Foxp3 activity. We acknowledge that in our suppression assays we did not observe an increase in suppressive capacity in cells treated with TIP60 inhibitor over control, when comparing the same number of cells. We contend that the increase in percentage at the end of the culture strongly suggests that Foxp3 activity might be more stable, which would be further enhanced by the fact that lysine acetylation precludes its ubiquitination and subsequent target for degradation.[64,65] We also acknowledge that TIP60-P300-Foxp3 might form a ternary complex and that our studies do not identify in which degree the modulatory

effects of TIP60 occur in the cytoplasm and the nucleus. The exact sequence of events that leads to Foxp3 acetylation will be the subject of further work.

To date, only a few small molecules have been described to promote Tregs, such as: Vitamin A, D, B3, B9, and bile acids derivatives.[13,66–68] These physiological metabolites, not newly synthetic drugs, play a key role in the inductions of mucosal Tregs, especially in intestinal inflammation, modulating the balance between Treg/Th17 cells. Our finding that TIP60 inhibitors can promote Treg inductions *in vitro* from naive T cells is of particular relevance for autologous Treg therapy, a strategy currently being evaluated for autoimmune disease and to prolong allograft survival.[11,12]

The mechanistic prediction put forward by the computational model and supported by our experimental data highlights an asymmetry in the fluxes of acetylation that lead to Foxp3 acetylation. Our findings reveal the importance of these asymmetries in understanding the acetylome and how they could be harnessed for therapeutic manipulation of Treg cell activity and function.

Limitations of the study

We acknowledge that all the proteins implicated in the TIP60-P300 mechanism described herein are highly regulated and are likely affected by deacetylases and ubiquitination. We also recognize that the FRET method presented to measure Foxp3 acetylation, despite being compatible with flow cytometry and studying the Foxp3 in its native state, does not allow us to discriminate specific acetylated Foxp3 lysines. In contrast, the peptide assay provides lysine-specific information but does not use the whole Foxp3 protein, thus making these assays complementary.

STAR★METHODS

Detailed methods are provided in the online version of this paper and include the following:

- KEY RESOURCES TABLE
- RESOURCE AVAILABILITY
  - Lead contact
  - Materials availability
  - Data and code availability
- EXPERIMENTAL MODEL AND STUDY PARTICIPANT DETAILS
  - Mice
  - Human subjects
- METHOD DETAILS
  - Lymphocyte isolation from the spleen and PBMCs
  - Flow cytometry, transcription factor and acetyltransferases staining
  - *In vitro* Treg cell inductions
  - Treg cell suppression assays
  - *In vitro* HAT and KAT assays
  - Peptide synthesis
  - Cell lysates KAT assays
  - Proximity ligation assay (PLA) for acetylated Foxp3
  - PLA image acquisition
  - PLA image analysis
  - ODE computational model
  - FRET flow cytometry
  - FRET flow cytometry analysis
  - FRET confocal imaging and analysis
  - Western Blot and immunoprecipitation
  - Quantitative RT-PCR
- QUANTIFICATION AND STATISTICAL ANALYSIS

SUPPLEMENTAL INFORMATION

Supplemental information can be found online at https://doi.org/10.1016/j.isci.2023.108491.

ACKNOWLEDGMENTS

The authors would like to acknowledge the contributions of Ana Fernández-Sesma and Dabeiba Bernal for providing buffy coats. Microscopy images were obtained at Microscopy CoRE and Advanced Bioimaging Center at the Icahn School of Medicine at Mount Sinai. The study was funded by NIH AI141710 awarded to M.F. and by grant PID2020-114256RB-I00 funded by MCIN/AEI/10.13039/501100011033 awarded to A.O.; and grants P21_00212 and A-FQM-386-UGR20 funded by FEDER/Junta de Andalucía-Consejería de Transformación Económica, Industria, Conocimiento y Universidades awarded to J.A.G.V.

AUTHOR CONTRIBUTIONS

M.F. and F.F.G. conceived the study. F.F.G., M.N., and N.M. performed the experiments and analyzed the data together with J.A.G.V., A.O., and M.F. G.V. developed the computational model and interpreted the results together with M.F.

DECLARATION OF INTERESTS

The authors declare no competing interests.

INCLUSION AND DIVERSITY

We support inclusive, diverse, and equitable conduct of research.

Received: March 23, 2023
Revised: August 12, 2023
Accepted: November 14, 2023
Published: November 19, 2023

REFERENCES

1. Waldmann, H., and Cobbold, S. (2001). Regulating the immune response to transplants. a role for CD4+ regulatory cells? Immunity *14*, 399–406.
2. Romano, M., Fanelli, G., Albany, C.J., Giganti, G., and Lombardi, G. (2019). Past, Present, and Future of Regulatory T Cell Therapy in Transplantation and Autoimmunity. Front. Immunol. *10*, 43.
3. Sakaguchi, S. (2005). Naturally arising Foxp3-expressing CD25+CD4+ regulatory T cells in immunological tolerance to self and non-self. Nat. Immunol. *6*, 345–352.
4. Kim, J.M., Rasmussen, J.P., and Rudensky, A.Y. (2007). Regulatory T cells prevent catastrophic autoimmunity throughout the lifespan of mice. Nat. Immunol. *8*, 191–197.
5. Buckner, J.H. (2010). Mechanisms of impaired regulation by CD4(+)CD25(+)FOXP3(+) regulatory T cells in human autoimmune diseases. Nat. Rev. Immunol. *10*, 849–859.
6. Hall, B.M. (2016). CD4+CD25+ T Regulatory Cells in Transplantation Tolerance: 25 Years On. Transplantation *100*, 2533–2547.
7. Rothstein, D.M., and Camirand, G. (2015). New insights into the mechanisms of Treg function. Curr. Opin. Organ Transplant. *20*, 376–384.
8. Wing, K., and Sakaguchi, S. (2010). Regulatory T cells exert checks and balances on self tolerance and autoimmunity. Nat. Immunol. *11*, 7–13.
9. Liu, R., Du, S., Zhao, L., Jain, S., Sahay, K., Rizvanov, A., Lezhnyova, V., Khaibullin, T., Martynova, E., Khaiboullina, S., and Baranwal, M. (2022). Autoreactive lymphocytes in multiple sclerosis: Pathogenesis and treatment target. Front. Immunol. *13*, 996469.
10. Tanaka, A., and Sakaguchi, S. (2017). Regulatory T cells in cancer immunotherapy. Cell Res. *27*, 109–118.
11. Gedaly, R., De Stefano, F., Turcios, L., Hill, M., Hidalgo, G., Mitov, M.I., Alstott, M.C., Butterfield, D.A., Mitchell, H.C., Hart, J., et al. (2019). mTOR Inhibitor Everolimus in Regulatory T Cell Expansion for Clinical Application in Transplantation. Transplantation *103*, 705–715.
12. Tang, Q., Leung, J., Peng, Y., Sanchez-Fueyo, A., Lozano, J.J., Lam, A., Lee, K., Greenland, J.R., Hellerstein, M., Fitch, M., et al. (2022). Selective decrease of donor-reactive T. Sci. Transl. Med. *14*, eabo2628.
13. Hang, S., Paik, D., Yao, L., Kim, E., Trinath, J., Lu, J., Ha, S., Nelson, B.N., Kelly, S.P., Wu, L., et al. (2019). Bile acid metabolites control T. Nature *576*, 143–148.
14. Kang, S.W., Kim, S.H., Lee, N., Lee, W.W., Hwang, K.A., Shin, M.S., Lee, S.H., Kim, W.U., and Kang, I. (2012). 1,25-Dihyroxyvitamin D3 promotes FOXP3 expression via binding to vitamin D response elements in its conserved noncoding sequence region. J. Immunol. *188*, 5276–5282.
15. Mucida, D., Park, Y., Kim, G., Turovskaya, O., Scott, I., Kronenberg, M., and Cheroutre, H. (2007). Reciprocal TH17 and regulatory T cell differentiation mediated by retinoic acid. Science *317*, 256–260.
16. van Loosdregt, J., and Coffer, P.J. (2014). Post-translational modification networks regulating FOXP3 function. Trends Immunol. *35*, 368–378.
17. Wang, L., Liu, Y., Beier, U.H., Han, R., Bhatti, T.R., Akimova, T., and Hancock, W.W. (2013). Foxp3+ T-regulatory cells require DNA methyltransferase 1 expression to prevent development of lethal autoimmunity. Blood *121*, 3631–3639.
18. Wang, L., Liu, Y., Han, R., Beier, U.H., Thomas, R.M., Wells, A.D., and Hancock, W.W. (2013). Mbd2 promotes foxp3 demethylation and T-regulatory-cell function. Mol. Cell Biol. *33*, 4106–4115.
19. Song, X., Li, B., Xiao, Y., Chen, C., Wang, Q., Liu, Y., Berezov, A., Xu, C., Gao, Y., Li, Z., et al. (2012). Structural and biological features of FOXP3 dimerization relevant to regulatory T cell function. Cell Rep. *1*, 665–675.
20. de Zoeten, E.F., Lee, I., Wang, L., Chen, C., Ge, G., Wells, A.D., Hancock, W.W., and Ozkaynak, E. (2009). Foxp3 processing by proprotein convertases and control of regulatory T cell function. J. Biol. Chem. *284*, 5709–5716.
21. van Loosdregt, J., Fleskens, V., Fu, J., Brenkman, A.B., Bekker, C.P.J., Pals, C.E.G.M., Meerding, J., Berkers, C.R., Barbi, J., Gröne, A., et al. (2013). Stabilization of the transcription factor Foxp3 by the deubiquitinase USP7 increases Treg-cell-suppressive capacity. Immunity *39*, 259–271.
22. Dahiya, S., Beier, U.H., Wang, L., Han, R., Jiao, J., Akimova, T., Angelin, A., Wallace, D.C., and Hancock, W.W. (2020). HDAC10 deletion promotes Foxp3. Sci. Rep. *10*, 424.
23. Liu, Y., Wang, L., Han, R., Beier, U.H., and Hancock, W.W. (2012). Two lysines in the forkhead domain of foxp3 are key to T regulatory cell function. PLoS One *7*, e29035.
24. Li, Z., Li, D., Tsun, A., and Li, B. (2015). FOXP3+ regulatory T cells and their functional regulation. Cell. Mol. Immunol. *12*, 558–565.
25. He, Z.X., Wei, B.F., Zhang, X., Gong, Y.P., Ma, L.Y., and Zhao, W. (2021). Current development of CBP/p300 inhibitors in the last decade. Eur. J. Med. Chem. *209*, 112861.
26. Katsumoto, T., Yoshida, N., and Kitabayashi, I. (2008). Roles of the histone acetyltransferase monocytic leukemia zinc finger protein in normal and malignant hematopoiesis. Cancer Sci. *99*, 1523–1527.
27. Jaiswal, B., Agarwal, A., and Gupta, A. (2022). Lysine Acetyltransferases and Their Role in AR Signaling and Prostate Cancer. Front. Endocrinol. *13*, 886594.
28. Yang, X.J. (2004). The diverse superfamily of lysine acetyltransferases and their roles in leukemia and other diseases. Nucleic Acids Res. *32*, 959–976.
29. Xiao, Y., Nagai, Y., Deng, G., Ohtani, T., Zhu, Z., Zhou, Z., Zhang, H., Ji, M.Q., Lough, J.W., Samanta, A., et al. (2014). Dynamic interactions between TIP60 and p300 regulate FOXP3 function through a structural switch defined by a single lysine on TIP60. Cell Rep. *7*, 1471–1480.
30. Li, B., Samanta, A., Song, X., Iacono, K.T., Bembas, K., Tao, R., Basu, S., Riley, J.L., Hancock, W.W., Shen, Y., et al. (2007). FOXP3 interactions with histone acetyltransferase and class II histone deacetylases are required for repression. Proc. Natl. Acad. Sci. USA *104*, 4571–4576.
31. van Loosdregt, J., Vercoulen, Y., Guichelaar, T., Gent, Y.Y.J., Beekman, J.M., van Beekum, O., Brenkman, A.B., Hijnen, D.J., Mutis, T., Kalkhoven, E., et al. (2010). Regulation of Treg functionality by acetylation-mediated Foxp3 protein stabilization. Blood *115*, 965–974.
32. Bin Dhuban, K., d'Hennezel, E., Nagai, Y., Xiao, Y., Shao, S., Istomine, R., Alvarez, F., Ben-Shoshan, M., Ochs, H., Mazer, B., et al. (2017). Suppression by human FOXP3. Sci. Immunol. *2*, eaai9297.
33. Zhang, X., Wu, J., and Luan, Y. (2017). Tip60: Main Functions and Its Inhibitors. Mini Rev. Med. Chem. *17*, 675–682.

34. Huang, M., Huang, J., Zheng, Y., and Sun, Q. (2019). Histone acetyltransferase inhibitors: An overview in synthesis, structure-activity relationship and molecular mechanism. Eur. J. Med. Chem. *178*, 259–286.
35. Ghizzoni, M., Wu, J., Gao, T., Haisma, H.J., Dekker, F.J., and George Zheng, Y. (2012). 6-alkylsalicylates are selective Tip60 inhibitors and target the acetyl-CoA binding site. Eur. J. Med. Chem. *47*, 337–344.
36. Coffey, K., Blackburn, T.J., Cook, S., Golding, B.T., Griffin, R.J., Hardcastle, I.R., Hewitt, L., Huberman, K., McNeill, H.V., Newell, D.R., et al. (2012). Characterisation of a Tip60 specific inhibitor, NU9056, in prostate cancer. PLoS One *7*, e45539.
37. Gao, C., Bourke, E., Scobie, M., Famme, M.A., Koolmeister, T., Helleday, T., Eriksson, L.A., Lowndes, N.F., and Brown, J.A.L. (2014). Rational design and validation of a Tip60 histone acetyltransferase inhibitor. Sci. Rep. *4*, 5372.
38. Mangan, P.R., Harrington, L.E., O'Quinn, D.B., Helms, W.S., Bullard, D.C., Elson, C.O., Hatton, R.D., Wahl, S.M., Schoeb, T.R., and Weaver, C.T. (2006). Transforming growth factor-beta induces development of the T(H)17 lineage. Nature *441*, 231–234.
39. Kwon, H.S., Lim, H.W., Wu, J., Schnölzer, M., Verdin, E., and Ott, M. (2012). Three novel acetylation sites in the Foxp3 transcription factor regulate the suppressive activity of regulatory T cells. J. Immunol. *188*, 2712–2721.
40. Yi, J., Huang, X., Yang, Y., Zhu, W.G., Gu, W., and Luo, J. (2014). Regulation of histone acetyltransferase TIP60 function by histone deacetylase 3. J. Biol. Chem. *289*, 33878–33886.
41. Fueyo-González, F., McGinty, M., Ningoo, M., Anderson, L., Cantarelli, C., Angeletti, A., Demir, M., Llaudó, I., Purroy, C., Marjanovic, N., et al. (2022). Interferon-β acts directly on T cells to prolong allograft survival by enhancing regulatory T cell induction through Foxp3 acetylation. Immunity *55*, 459–474.e457.
42. Jiao, J., Han, R., Hancock, W.W., and Beier, U.H. (2017). Proximity Ligation Assay to Quantify Foxp3 Acetylation in Regulatory T Cells. Methods Mol. Biol. *1510*, 287–293.
43. Spence, M.T., and Johnson, I.D. (2010). The Molecular Probes Handbook: A Guide to Fluorescent Probes and Labeling Technologies (Life Technologies Corporation).
44. Padilla-Parra, S., and Tramier, M. (2012). FRET microscopy in the living cell: different approaches, strengths and weaknesses. Bioessays *34*, 369–376.
45. Ruiz-Arias, A., Jurado, R., Fueyo-González, F., Herranz, R., Gálvez, N., González-Vera, J.A., and Orte, A. (2022). A FRET pair for quantitative and superresolution imaging of amyloid fibril formation. Sensor. Actuator. B Chem. *350*, 130882.
46. Zhao, S., Xu, W., Jiang, W., Yu, W., Lin, Y., Zhang, T., Yao, J., Zhou, L., Zeng, Y., Li, H., et al. (2010). Regulation of cellular metabolism by protein lysine acetylation. Science *327*, 1000–1004.
47. Sterner, D.E., and Berger, S.L. (2000). Acetylation of histones and transcription-related factors. Microbiol. Mol. Biol. Rev. *64*, 435–459.
48. Goel, A., and Janknecht, R. (2003). Acetylation-mediated transcriptional activation of the ETS protein ER81 by p300, P/CAF, and HER2/Neu. Mol. Cell Biol. *23*, 6243–6254.
49. Xiong, Y., and Guan, K.L. (2012). Mechanistic insights into the regulation of metabolic enzymes by acetylation. J. Cell Biol. *198*, 155–164.
50. Liu, Y., Wang, L., Predina, J., Han, R., Beier, U.H., Wang, L.C.S., Kapoor, V., Bhatti, T.R., Akimova, T., Singhal, S., et al. (2013). Inhibition of p300 impairs Foxp3$^+$ T regulatory cell function and promotes antitumor immunity. Nat. Med. *19*, 1173–1177.
51. Liu, Y., Wang, L., Han, R., Beier, U.H., Akimova, T., Bhatti, T., Xiao, H., Cole, P.A., Brindle, P.K., and Hancock, W.W. (2014). Two histone/protein acetyltransferases, CBP and p300, are indispensable for Foxp3+ T-regulatory cell development and function. Mol. Cell Biol. *34*, 3993–4007.
52. Ononye, O.E., and Downey, M. (2022). Posttranslational regulation of the GCN5 and PCAF acetyltransferases. PLoS Genet. *18*, e1010352.
53. Bowers, E.M., Yan, G., Mukherjee, C., Orry, A., Wang, L., Holbert, M.A., Crump, N.T., Hazzalin, C.A., Liszczak, G., Yuan, H., et al. (2010). Virtual ligand screening of the p300/CBP histone acetyltransferase: identification of a selective small molecule inhibitor. Chem. Biol. *17*, 471–482.
54. Henry, R.A., Kuo, Y.M., Bhattacharjee, V., Yen, T.J., and Andrews, A.J. (2015). Changing the selectivity of p300 by acetyl-CoA modulation of histone acetylation. ACS Chem. Biol. *10*, 146–156.
55. Tao, R., de Zoeten, E.F., Ozkaynak, E., Chen, C., Wang, L., Porrett, P.M., Li, B., Turka, L.A., Olson, E.N., Greene, M.I., et al. (2007). Deacetylase inhibition promotes the generation and function of regulatory T cells. Nat. Med. *13*, 1299–1307.
56. Beier, U.H., Wang, L., Han, R., Akimova, T., Liu, Y., and Hancock, W.W. (2012). Histone deacetylases 6 and 9 and sirtuin-1 control Foxp3+ regulatory T cell function through shared and isoform-specific mechanisms. Sci. Signal. *5*, ra45.
57. Lemercier, C., Legube, G., Caron, C., Louwagie, M., Garin, J., Trouche, D., and Khochbin, S. (2003). Tip60 acetyltransferase activity is controlled by phosphorylation. J. Biol. Chem. *278*, 4713–4718.
58. Dimitrova, Y.N., Gutierrez, J.A., and Huard, K. (2023). It's ok to be outnumbered - sub-stoichiometric modulation of homomeric protein complexes. RSC Med. Chem. *14*, 22–46.
59. Felix, J., Weinhäupl, K., Chipot, C., Dehez, F., Hessel, A., Gauto, D.F., Morlot, C., Abian, O., Gutsche, I., Velazquez-Campoy, A., et al. (2019). Mechanism of the allosteric activation of the ClpP protease machinery by substrates and active-site inhibitors. Sci. Adv. *5*, eaaw3818.
60. Merdanovic, M., Burston, S.G., Schmitz, A.L., Köcher, S., Knapp, S., Clausen, T., Kaiser, M., Huber, R., and Ehrmann, M. (2020). Activation by substoichiometric inhibition. Proc. Natl. Acad. Sci. USA *117*, 1414–1418.
61. Konagaya, Y., Terai, K., Hirao, Y., Takakura, K., Imajo, M., Kamioka, Y., Sasaoka, N., Kakizuka, A., Sumiyama, K., Asano, T., and Matsuda, M. (2017). A Highly Sensitive FRET Biosensor for AMPK Exhibits Heterogeneous AMPK Responses among Cells and Organs. Cell Rep. *21*, 2628–2638.
62. Lim, J., Petersen, M., Bunz, M., Simon, C., and Schindler, M. (2022). Flow cytometry based-FRET: basics, novel developments and future perspectives. Cell. Mol. Life Sci. *79*, 217.
63. Schilling, B., Meyer, J.G., Wei, L., Ott, M., and Verdin, E. (2019). High-Resolution Mass Spectrometry to Identify and Quantify Acetylation Protein Targets. Methods Mol. Biol. *1983*, 3–16.
64. Dong, Y., Yang, C., and Pan, F. (2021). Post-Translational Regulations of Foxp3 in Treg Cells and Their Therapeutic Applications. Front. Immunol. *12*, 626172.
65. Chen, Z., Barbi, J., Bu, S., Yang, H.Y., Li, Z., Gao, Y., Jinasena, D., Fu, J., Lin, F., Chen, C., et al. (2013). The ubiquitin ligase Stub1 negatively modulates regulatory T cell suppressive activity by promoting degradation of the transcription factor Foxp3. Immunity *39*, 272–285.
66. Zeng, H., and Chi, H. (2015). Metabolic control of regulatory T cell development and function. Trends Immunol. *36*, 3–12.
67. Fisher, S.A., Rahimzadeh, M., Brierley, C., Gration, B., Doree, C., Kimber, C.E., Plaza Cajide, A., Lamikanra, A.A., and Roberts, D.J. (2019). The role of vitamin D in increasing circulating T regulatory cell numbers and modulating T regulatory cell phenotypes in patients with inflammatory disease or in healthy volunteers: A systematic review. PLoS One *14*, e0222313.
68. Tejón, G., Manríquez, V., De Calisto, J., Flores-Santibáñez, F., Hidalgo, Y., Crisóstomo, N., Fernández, D., Sauma, D., Mora, J.R., Bono, M.R., and Rosemblatt, M. (2015). Vitamin A Impairs the Reprogramming of Tregs into IL-17-Producing Cells during Intestinal Inflammation. BioMed Res. Int. *2015*, 137893.
69. Schindelin, J., Arganda-Carreras, I., Frise, E., Kaynig, V., Longair, M., Pietzsch, T., Preibisch, S., Rueden, C., Saalfeld, S., Schmid, B., et al. (2012). Fiji: an open-source platform for biological-image analysis. Nat. Methods *9*, 676–682.
70. Bordería, A.V., Hartmann, B.M., Fernandez-Sesma, A., Moran, T.M., and Sealfon, S.C. (2008). Antiviral-activated dendritic cells: a paracrine-induced response state. J. Immunol. *181*, 6872–6881.
71. Yuen, T., Wurmbach, E., Pfeffer, R.L., Ebersole, B.J., and Sealfon, S.C. (2002). Accuracy and calibration of commercial oligonucleotide and custom cDNA microarrays. Nucleic Acids Res. *30*, e48.

STAR★METHODS

KEY RESOURCES TABLE

REAGENT or RESOURCE	SOURCE	IDENTIFIER
Antibodies		
PE-Cy7 anti-mouse CD4 antibody antibody	eBiosciences	Cat# 25-0041-82 RRID:AB_469576
PerCP Cy5.5 anti-mouse CD45 antibody	Invitrogen	Cat# 45-0451-82 RRID:AB_1107002
FITC anti-mouse CD3 antibody	Invitrogen	Cat# 11-0031-85 RRID:AB_464883
TIP60 (C-7) AF488	SantaCruz	Cat# Sc-166323
P300 (F-4) AF488	SantaCruz	Cat# Sc-48343
TIP60 (C-7) AF546	SantaCruz	Cat# Sc-166323
BV450 anti-human Foxp3	eBiosciences	Cat# 48-4776-42 RRID:AB_1834364
eFluor450 anti-mouse Foxp3	eBiosciences	Cat# 48-5773-82 RRID:AB_1518812
A488 anti-mouse Foxp3	eBiosciences	Cat# 53-5773-82 RRID:AB_1518812
FITC anti-mouse CD25 antibody	BD Biosciences	Cat# 553072 RRID:AB_394604
APC anti-annexin V antibody	BD Biosciences	Cat#550474 RRID:AB_2868885
Mouse anti-mouse anti-human Foxp3 antibody PLA assay	eBioscience	Cat# 14-7979-80 RRID:AB_468499
Rabbit anti-mouse anti-human acetylated lysines PLA assay	CellSignaling	Cat# 9441 RRID:AB_331805
αCD3 mouse	BioLegend	Cat# 100201 RRID:AB_312658
αCD3 human	BD Biosciences	Cat# 566685
FITC anti-human Foxp3	eBiosciences	Cat# 11-4777-42 RRID:AB_1518812
PerCP Cy5.5 anti-human CD4 antibody	BD Biosciences	Cat# 552838 RRID:AB_394488
APC anti-human CD25 antibody	eBiosciences	Cat# 17-0259-42 RRID:AB_1582219
PE anti-human CD127 antibody	BD Biosciences	Cat# 557938 RRID:AB_2296056
FITC anti-human CD4 antibody	eBiosciences	Cat# 11-0042-86 RRID:AB_464898
Anti-Acetyl Lysine-HRP	Immunechem	Cat# ICP0381
Chemical, peptides and recombinant proteins		
Recombinant murine IL-2	Peprotech	Cat# 212-12
Recombinant TGFβ1	Peprotech	Cat# 100-21C
Recombinant human IL-2	BD Pharmingen	Cat# 554603
CellTrace violet Cell Proliferation	Thermofisher	Cat# C34557
C646	SigmaAldrich	Cat# SML0002
NU 9056	Tocris	Cat#4903
MG 149	MedChemExpress	Cat#HY-15887
TH 1834	axonmedchem	Cat#2339
Ivermectin	SigmaAldrich	Cat#18898
KAT5 (TIP60), Active	SigmaAldrich	Cat#SRP0706
Recombinant P300 protein	ActiveMotif	Cat#31124
Histone Acetyltransferase (HAT) Activity Assay Kit	SigmaAldrich	Cat#EPI001-1KT
Dye Removal Columns	ThermoScientific	Cat#22858
AlexaFluor488 Carboxylic acid, succinimil ester	Invitrogen	Cat#A20000
AlexaFluor55 Carboxylic acid, succinimil ester	Invitrogen	Cat#A20009
eFluor 780 Fixable viability dye	eBioscience	Cat# 65-0865-14
ACK lysis buffer	Roche	Cat# 11814389001
5X RIPA Buffer	ThermoScientific	Cat# J62524.AE
Pierce BCA protein assay	ThermoScientific	Cat# 23228

(*Continued on next page*)

Continued

REAGENT or RESOURCE	SOURCE	IDENTIFIER
Protein G MagBeads	GenScript	Cat# L00274
Laemmli SDS sample Buffer, reducing (6x)	Millipore	Cat# J61337.AC
Immobilon®- P Transfer Membrane (Pore 0.45µm)	Millipore	Cat# IPVH00010
Immobilon® Western Chemiluminescent HRP Substrate	ThermoScientific	Cat# WBKLS0100
TritonX-100	Immunechem	Cat# A16046.AE
AffinityScript MultiTemp RT	Agilent	Cat# 600105
PlatinumTaq DNA polymerase	Invitrogen	Cat# 11804011
SYBR Green	Invitrogen	Cat# 4402959
Critical commercial assays		
EasySep™ Mouse Naïve $CD4^+$ T Cell Isolation Kit	STEMCELL Technologies	Cat# 19765
EasySep™ Human Naïve $CD4^+$ T Cell Isolation Kit	STEMCELL Technologies	Cat# 19555
EasySep™ Mouse T Cell Isolation Kit	STEMCELL Technologies	Cat# 19851
EasySep™ Mouse CD90.2 Positive Selection Kit II	STEMCELL Technologies	Cat# 18951
aCD3/aCD28 stimulating beads murine	Gibco	Cat# 11-161D
aCD3/aCD28 stimulating beads human	Gibco	Cat# 11-456D
Duolink™ *In Situ* PLA® Probe Anti-Mouse PLUS	Sigma Aldrich	Cat# DUO92001
Duolink™ *In Situ* PLA® Probe Anti-Rabbit MINUS	Sigma Aldrich	Cat# DUO92005
Duolink™ *In Situ* Detection Reagents Red	Sigma Aldrich	Cat# DUO92008
Duolink™ *In Situ* Mounting Medium with DAPI	Sigma Aldrich	Cat# DUO82040
Intracellular/transcription factor staining buffer kit	eBiosciences	Cat# 00-5523-00
Experimental models: Organisms/strains		
C57BL/6J (B6)	The Jackson Laboratory	Stock No: 000664
BALB/cJ (BALB/c)	The Jackson Laboratory	Stock No: 000651
Software and algorithms		
Computational model mechanism of TIP60/P300 heteromer formation and Foxp3 acetylation	Fribourg Lab (this manuscript)	https://doi.org/10.5281/zenodo.10067436
FCS Express 7	*De Novo* Software	N/A
Matlab	Mathworks	N/A
SpotCountPLA Matlab Toolbox	Fribourg Lab	https://doi.org/10.5281/zenodo.5794212
ImageJ	NIH	N/A
Rstudio	Rstudio.com	N/A
SymphoTime 64	PicoQuant	N/A

RESOURCE AVAILABILITY

Lead contact

Further information and requests for resources and reagents should be directed to and will be fulfilled by the Lead Contact, Miguel Fribourg (miguel.fribourg@mssm.edu).

Materials availability

We will provide Foxp3-AF488 and AcK-AF555 conjugated antibodies to requesting labs that have received approval for the use of these mice via an MTA with the Icahn School of Medicine at Mount Sinai.

Data and code availability

- All original code and computational has been deposited in Zenodo. The DOI is listed in the key resources table.
- Any additional information required to reanalyze the data reported in this paper is available from the lead contact upon request.

EXPERIMENTAL MODEL AND STUDY PARTICIPANT DETAILS

Mice

Male and female C57BL/6 (H-2Kb) and BALB/c (H-2Kd) were purchased from The Jackson Laboratory (stocks #000664 and #000651, respectively) and bred at mouse facilities of the Icahn School of Medicine at Mount Sinai. Foxp3-GFP mice (Figure 1) was purchased from the Jackson Laboratory (stocks #023800). Data depicted in the figures include male and female mice as we used both male and female mice for Treg cell inductions (Figures 1, 2, 3, 4, and 5), suppression assays (Figure 1), HAT and KAT assays (Figure 2), FRET experiments (Figures 3 and 5), and WB experiments (Figure 6). This study was carried out in strict accordance with the recommendations in the Guide for the Care and Use of Laboratory Animals and under the protocol (IACUC-2018-2) approved by the Institutional Animal Care and Use Committee of the Icahn School of Medicine at Mount Sinai. All animals were housed in the animal facilities at the Icahn School of Medicine at Mount Sinai.

Human subjects

For experiments in human cells (Figure 7) we used peripheral blood mononuclear cells (PBMCs) from buffy coats obtained from anonymous donors to the New York Blood Bank.

METHOD DETAILS

Lymphocyte isolation from the spleen and PBMCs

Spleens were harvested in PBS and mechanically disaggregated through a mesh strainer (70 μm) with the aid of the back of a syringe plunger. PBS was decanted after centrifugation and red blood cells lysed (ACK lysis buffer, 2 min at room temperature, Roche). Cells were then centrifuged, re-suspended in PBS and filtered again through a 70 μm nylon mesh. The isolated single-cell suspension of enriched either spleen or PBMCs leukocytes was processed for different assays, or used to isolate naive $CD4^+$ T cells naive T cells using magnetic separation (EasySep Mouse or Human Naive $CD4^+$ T cell Isolation Kit, STEMCELL Kit) for Treg cell induction cultures.

Flow cytometry, transcription factor and acetyltransferases staining

Cells were evaluated for surface antigen expression following incubation with fluorescently conjugated antibodies in PBS or a buffer consisting of 2% rat serum 2 mM EDTA according to the manufacturer's instructions. For Foxp3, AcK, p300, and TIP60 staining, cells were permeabilized using an intracellular/transcription factor staining kit (eBiosciences) and stained with Foxp3, AcK, p300, and TIP60 antibodies. Data were acquired on a 3-laser FACSLyric flow cytometer (BD bioscience) and analyzed using FCS express 7 software.

In vitro Treg cell inductions

For *in vitro* Treg cell inductions either T $CD4^+$ naïve or Human peripheral blood mononuclear cells (PBMCs) were isolated from spleens or buffy coats by Ficoll density gradient centrifugation (Histopaque, SigmaAldrich) at 490g. Naïve $CD4^+$ T cells were enriched from murine splenocytes (CD44loCD62hi) or human peripheral blood mononuclear cells (CD45RA+CD45RO-) (EasySep™ Mouse Naïve $CD4^+$ T Cell Isolation Kit, EasySep™ Human Naïve $CD4^+$ T Cell Isolation Kit, respectively, STEMCELL Technologies) and their purity checked by flow cytometry. Mouse cultures: 200,000 naïve $CD4^+$ T cells were incubated with IL-2 (2.75 ng/ml, Peprotech), TGFβ (0.7 ng/ml, Peprotech) and stimulated with αCD3/αCD28 (15 μl/million cells, Gibco) (polyclonal). Human cultures: 200,000 naïve $CD4^+$ T cells were cultured with IL-2 (100 U/ml, BD Pharmingen), TGFβ (3 ng/ml, Peprotech) and stimulated with αCD3/αCD28 (15 μl/million cells, Gibco).

Treg cell suppression assays

Mice. 200,000 conventional B6 T cells (EASYSEP) labeled with a cell tracker (CellTrace violet) were stimulated by αCD3/αCD28 in the presence of different amounts of induced Treg cell with αCD3/αCD28 (polyclonal), previously sorted as Foxp3-GFP+ (Foxp3-GFP mice) (Figure 1). *Human*. 200,000 PBMCs labeled with CellTrace violet were stimulated with αCD3/αCD28 (1ng/ml, BD Biosciences) in the presence of different amounts of polyclonally induced Treg cell, previously sorted as $CD4^+CD25^{hi}CD127^-$ (Figure 6). Both for mouse and human suppression assays, the percentage of proliferating cells was determined by flow cytometry based on cell tracker dilution 5 days after stimulation.

In vitro HAT and KAT assays

HAT and KAT activity was determined using HAT assay according to the manufacturer's instructions (EPI001-1kt, Sigma-Aldrich, H3 peptide 1-21 sequence ARTKQTARKSTGGKAPRKQLA) using either KAT5 (TIP60 active recombinant protein, #SRP0706, Sigma-Aldrich, St.Louis, MO, USA) or recombinant P300 protein (#81158, Active Motif, California, USA) at 10 nM (Figure 2). KAT activity measurements were adapted from HAT assay to measure Foxp3 peptide acetylation replacing histone peptide sequence to Foxp3 peptide sequence described below. Both, HAT and KAT assays were performed in HAT assay buffer in the presence or absence of TIP60 inhibitors for 2 hours at 37°C. Reactions were stopped and measured by spectrophotometer according to the manufacturer's instructions.

Peptide synthesis

Foxp3 peptide (LAGKMALAKAPS) was purchased from GenScript, (New Jersey, USA) (Figure 2).

Cell lysates KAT assays

Cells extracts were obtained from Treg cell inductions in the presence or absence of TIP60 inhibitors at day 5 using NE-PER Nuclear and Cytoplasmic Extraction Reagents (#78833, Thermo Scientific, USA). KAT activity measurements from combined nuclear and cytoplasmic extracts were determined using KAT assay according to the protocol indicated above (Figure 2). Cell extracts were standardized based on protein concentration, measured through NanoDrop™ OneC Microvolume UV-Vis Spectrophotometer. The final protein concentration utilized to KAT activity measurements from the Treg cell extracts was 2.5 μg/mL. The enzymatic reaction was performed for 2 hours.

Proximity ligation assay (PLA) for acetylated Foxp3

Cells from mouse Treg cell induction cultures in presence or absence of MG149 (25 μM) were harvested and cultured for 2 hours at 37°C in 50-100 μl drops containing 50,000 cells on top of coverslips previously coated with poly-D-lysine and laminin. Coverslips were then washed and the cells attached to it fixed by immersion in 3.7% PFA for 10 min at room temperature, and permeabilized by immersion in 70% ethanol for 20 min. The proximity ligation assay was then performed following the manufacturer's recommendations and the particularizations described in the protocol from Hancock and Beier31 using primary antibodies against Foxp3 (raised in mouse, eBiosciences) and acetylated lysines (raised in rabbit, Cell Signaling), Duolink™ *In Situ* PLA® Probe Anti-Mouse PLUS Reagents (Sigma Aldrich) together with Anti-Rabbit MINUS (Sigma Aldrich) and Duolink™ *In Situ* Detection Reagents Red. Finally, the coverslips were mounted on slides using a DAPI-containing mounting medium (Figure 3).

PLA image acquisition

Cells were imaged with and upright epifluorescence microscope, Axioplan 2 (Zeiss), with a 100x oil immersion objective and a numerical aperture of 1.3. The microscope was controlled by AxioVision software and was equipped with a Zeiss AxioCam MRm camera. Images were acquired in brightfield. The laser exposure time for the red PLA probes was adjusted for every experiment and ranged between 1 and 2 seconds. 20-25 fields were obtained from each coverslip with 2-10 per field. Multiple coverslip per mouse and per treatment were analyzed per experiment. Control experiments were performed with only one primary antibody (either Foxp3 or acetylated lysines) to establish background levels and specificity of the signal.

PLA image analysis

The nuclear image from the blue channel (DAPI) and the spot image from the red channel (PLA) are processed separately. Briefly, both the nuclear image and the spot image are (i) normalized to maximum intensity, (ii) contrast-enhanced using adaptive histogram equalization, (iii) and a threshold applied to them to eliminate background. To segment the cells, we utilized an extended maxima transform followed by a watershed transform to define a region of influence for each cell. The spot image was sharpened using the unsharp masking technique, and the spots identified by labeling connected components in a binary version of the image. The images with the regions of influence and with the spots were overlaid and each spot assigned to the corresponding cell provided it was at a distance shorter than 150 pixels from the nucleus of the cell. To establish fair comparisons of levels of Foxp3 acetylation between treatments, cells with zero spots were excluded from each group reasoning that they were not Foxp3+. In Treg cell induction experiments, at least 40% of the cells had at least one spot. The image analysis was implemented in Matlab and is accessible at Matlab Central (https://www.mathworks.com/matlabcentral/fileexchange/103185-spotcountpla).

ODE computational model

The ODE model of P300 and TIP60 effects of Foxp3 was implemented and simulated in Matlab. Please refer to supplemental information for details on model equations parameters and other details. The model will be made publicly available upon publication of the article at the BioModel bioarchive (http:/ebi.ac.uk/biomodels/).

FRET flow cytometry

Cells were harvested at the end 5-day mouse or human Treg cell induction cultures in the presence or absence of TIP60 inhibitors (NU9056, MG149, and TH1834 for mice, MG149 for humans) and were surface staining with αCD4 antibody together with a fixable viability dye (or an α−Annexin V antibody). For Foxp3, Acetylated lysines (AcK), P300, and TIP60 intracellular staining, cells were fixed/permeabilized using an intracellular/transcription factor staining kit (eBiosciences). Each biological sample was divided into 3 for distinct staining: (i) FRET donor antibody alone (Foxp3, P300, or TIP60) labeled with AF488, (ii) FRET acceptor antibodies alone labeled with AF555 (AcK, TIP60, or CD3) and (iii) both together. Antibodies were labeled with the appropriate fluorophores using a protein labeling kit (#A20174, Thermo Fisher Scientific, USA). Samples were analyzed in an Attune NxT flow cytometer (Thermo Fisher Scientific) acquiring either the donor (excitation 488 nm; detection, green; blue1 in Attune) and acceptor channel (excitation 555 nm; detection, yellow; yellow 1 in Attune) alone, or the donor and FRET (excitation 488 nm; detection; blue 4 in Attune) channels together. Additional controls swapping donor and acceptor antibody-proteins and with non-colocalized proteins were performed. A full list of antibodies used are available in the *Reagents* section.

FRET flow cytometry analysis

Flow cytometry data and analyzed using FCS express software.

For FRET efficiency calculation flow cytometry.fcs files were parsed using scripts programmed in R. For each cell the apparent FRET efficiency was obtained as:

$$\%FRET\ Eff. = \frac{(Acceptor\ Intensity - Mean\ Background\ Acceptor\ Intensity)*100}{Donor\ Intensity - Mean\ Background\ Donor\ Intensity} \quad \text{(Equation 1)}$$

where the Mean Background Acceptor and Donor Intensities were estimated from the counterpart mono-stained samples restricted to $CD4^+$ cells. All subtracted intensities which resulted in a negative number were set to 0 to avoid negative FRET efficiencies. A channel with %FRET efficiency with the calculated value for each cell was created in the.fcs file and the mean %FRET efficiency for each subcompartment (Foxp3- and Foxp3+) cells obtained using conventional gating in FCS Express.

FRET confocal imaging and analysis

Cells from human Treg cell induction cultures in presence or absence of MG149 (25 μM) were harvested and cultured for 2 hours at 37°C in 50-100 μl drops containing 50,000 cells on top of coverslips previously coated with poly-D-lysine and laminin. Coverslips were then washed and the cells attached to it fixed by immersion in 3.7% PFA for 10 min at room temperature, and permeabilized by immersion in 70% ethanol for 20 min. Foxp3 was stained with the primary antibodies against Foxp3 labelled with AF488 (eBiosciences) as the donor and acetylated lysines labelled with AF555 (Cell Signaling) as an acceptor. Confocal images were obtained with a Leica TCS SP8 microscope in the AF488 and AF555 (FRET) channel exciting with the 488nm laser.

All image analysis was performed using SymphoTime 64 (PicoQuant) and ImageJ distribution FIJI.[69] The FRET efficiency reconstructed image was obtained pixelwise by applying the same Equation 1 described above. An intensity threshold in the donor channel was applied to select Foxp3+ cells, including pixels with intensity above 25 photons. For cellwise analysis, obtaining the average %FRET value of individual cells in Figure 6D, a segmentation procedure was carried out using the *Analyze Particles* script in FIJI.

Western Blot and immunoprecipitation

Cells were harvested on day 5 of Treg induction cultures and were lysed in 1x RIPA buffer (Thermo Scientific). After centrifugation, the soluble fractions were collected and protein concentration was determined using Pierce BCA protein assay (Thermo Scientific). Equal protein amounts were then incubated with αTIP60 or αP300 or αFoxp3 labeled-protein G MagBeads (Genscript) overnight at 4°C. The precipitates were then washed three times with 0.1% TritonX-100 buffer (Thermo Scientific) and boiled for 5 min with Laemmli SDS sample buffer (Thermo Scientific). Samples (or TIP60 protein for *in vitro* biochemical assays) were analyzed by SDS-PAGE, transferred to polyvinylidene difluoride membrane (Millipore), and probed with the respective antibodies. Immunocomplexes were detected using Immobilon Western Chemiluminescent horseradish peroxidase (HRP) Substrate (Millipore). Membranes were imaged using Li-Cor Odyssey Fc (LiCor Biosciences) and quantified using ImageJ.

Quantitative RT-PCR

RNA expression was quantified using quantitative RT-PCR. cDNA was synthesized from total RNA using AffinityScript MultiTemp RT (Agilent) with an oligo(dT)18 primer. Real-time PCR was performed using PlatinumTaq DNA polymerase (Invitrogen) and SYBR Green (Invitrogen) on an ABI7900HT thermal cycler (Applied Biosystems), as described previously.[70] A robust global normalization algorithm, using expression levels of the housekeeping genes ribosomal protein S11 (*Rps11*), β-actin (*Actb*), and α-tubulin (*Tuba*), was used for all experiments, as described elsewhere.[70,71] In brief, all crossing threshold values (Ct) were first adjusted by median difference of all samples from *Actb*. Each individual sample was then further corrected by the median crossing threshold value of the three corrected housekeeping control for that sample and the corrected ΔCt obtained.

QUANTIFICATION AND STATISTICAL ANALYSIS

Foxp3 acetylation (spot count, no normal distribution of the data assumed) were compared between groups using a Mann Whitney test. Suppression data were fitted to a one-site total binding curve followed by an extra-sum-of-squares F test to determine if the curves are different. For the rest of the comparisons we applied unpaired t-tests (two groups) or one-way ANOVA followed by Tukey's post-hoc HSD test (multiple groups). All analyses were done using Prism (GraphPad Software). In all legends and figures, mean ± S.E.M. is shown, and *$p < 0.05$, #$p < 0.01$,and n.s., non-significant.